Journal of Inorganic and General Chemistry
ZAAC
Zeitschrift für anorganische und allgemeine Chemie
www.zaac.wiley-vch.de
RESEARCH ARTICLE

DOI: 10.1002/zaac.202200334

Special Collection

A Stable Crystalline N-Heterocyclic Carbene with a 1,1′-Ferrocenylene Backbone and Benzylic *N*-Substituents

Julian Zinke,[a] Clemens Bruhn,[a] and Ulrich Siemeling*[a]

Dedicated to Prof. Sjoerd Harder on the Occasion of his 60th Birthday

Two ferrocene-based NHCs of the type fc[(NR)$_2$C:] (**1**^{R}; fc = 1,1′-ferrocenylene) containing benzylic *N*-substituents were synthesised from the corresponding formamidinium compounds **1**^{R}H-[BF$_4$] by reaction with LiN(SiMe$_3$)$_2$. In the case of R = CH$_2$Ph (Bn), the carbene was characterised through trapping reactions with sulfur and selenium, which afforded fc[(NBn)$_2$CS] (**1**^{Bn}S) and fc[(NBn)$_2$CSe] (**1**^{Bn}Se), respectively. A thermally stable carbene was obtained with R = CH$_2$Mes (Bn*). Its reaction with sulfur and selenium afforded fc[(NBn*)$_2$CS] (**1**^{Bn*}S) and fc[(NBn*)$_2$CSe] (**1**^{Bn*}Se), respectively. Its reaction with [Rh(μ-Cl)(COD)]$_2$ (COD = cycloocta-1,5-diene), followed by substitution of the COD ligand by CO, furnished *cis*-[RhCl(CO)$_2$(**1**^{Bn*})]. In combination with IR data of *cis*-[RhCl(CO)$_2$(**1**^{Bn*})], NMR data of **1**^{Bn*}H[BF$_4$], **1**^{Bn*} and **1**^{Bn*}Se indicate that **1**^{Bn*} is substantially more nucleophilic and more electrophilic than conventional Arduengo carbenes, exhibiting an ambiphilicity similar to that of CAACs. The crystal structures of the formamidinium salts **1**^{R}HX (X = [BF$_4$], R = Bn, Bn*; X = Cl, R = Bn*), of the carbene **1**^{Bn*} and its Au^I complex [AuCl(**1**^{Bn*})] as well as of the sulfur and selenium derivatives **1**^{R}E (E = S, Se; R = Bn, Bn*), the Rh^I complexes *cis*-[RhCl(CO)$_2$(**1**^{R})] (R = Bn, Bn*) and the Cu^I complex [CuBr(**1**^{Bn})] were determined by single-crystal X-ray diffraction (XRD). In addition, the crystals structures of the diimine fc(N=CHMes)$_2$ and the diamine fc(NHBn*)$_2$ were also determined by XRD.

Introduction

1,1′-Ferrocenylene-bridged N-heterocyclic carbenes (fcNHCs) of the type fc[(NR)$_2$C:] (**1**^{R}, fc = 1,1′-ferrocenylene; Figure 1) were introduced in 2008 by Bielawski, who demonstrated that the fc backbone of fcNHCs can be utilised for redox-switching of their electronic ligand properties,[1] thus allowing applications in redox-tunable metal complex catalysis.[2] From a formal point of view, fcNHCs are expanded-ring N-heterocyclic carbenes (erNHCs)[3] with a six-membered heterocycle. The N–C–N angles of erNHCs are significantly larger than those of their five-membered ring counterparts (100–106°)[4] and, depending on the ring size, may even come close to values observed for acyclic diaminocarbenes (ca. 121°).[5] As a consequence, erNHCs exhibit a higher steric impact together with a more pronounced ambiphilicity, and hence higher reactivity and lower thermal stability, than standard five-membered NHCs.[6] The *N*-substituents employed by Bielawski (R = methyl, isobutyl, phenyl) afforded carbenes too unstable for isolation, thus prohibiting a study of the free fcNHCs. Utilising bulkier *N*-substituents, viz. neopentyl, 2-adamantyl and *tert*-butyl, we have been able to prepare thermally stable congeners,[7] which turned out to exhibit a pronounced ambiphilicity similar to that of cyclic (alkyl)(amino)carbenes (CAACs), thus allowing the activation of fundamentally important small molecules such as, for example, CO and NH$_3$.[7b,8,9] The neopentyl substituent proved to be particularly useful in this work, being beneficial for the thermal stability of the carbene as well as for the solubility and crystallinity of the carbene and its precursors. This prompted us to address other primary alkyl substituents. We started with benzylic ones, since we surmised that replacement of the neopentyl (CH$_2$*t*Bu) *tert*-butyl subunit by suitable aryl groups should also lead to advantageous properties in this context. We have already published results for aryl = *p*-C$_6$H$_4$–X (X = OMe, NMe$_2$). These groups lead to fcNHCs too unstable for isolation,

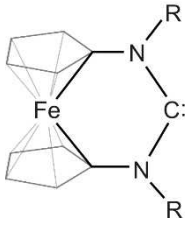

Figure 1. Structure of fcNHCs **1**^{R} (drawn in a way that highlights the six-membered ring structure formally present in these [3]ferrocenophane-type compounds).

[a] J. Zinke, C. Bruhn, Prof. Dr. U. Siemeling
Institute of Chemistry
University of Kassel
Heinrich-Plett-Str. 40, 34132 Kassel, Germany
Fax: +49-561-8044777
E-mail: siemeling@uni-kassel.de

Supporting information for this article is available on the WWW under https://doi.org/10.1002/zaac.202200334

This article is part of a Special Collection dedicated to Professor Sjoerd Harder on the occasion of his 60th birthday. Please see our homepage for more articles in the collection.

© 2022 The Authors. Zeitschrift für anorganische und allgemeine Chemie published by Wiley-VCH GmbH. This is an open access article under the terms of the Creative Commons Attribution License, which permits use, distribution and reproduction in any medium, provided the original work is properly cited.

which, however, could be efficiently trapped by complexation at rhodium(I) or by reaction with elemental selenium.[10] We here describe our work with the pristine benzyl substituent (CH_2Ph, Bn) and its mesityl-containing homologue CH_2Mes (Bn*).

Results and Discussion

The synthesis of the target fcNHCs $\mathbf{1}^{Bn}$ and $\mathbf{1}^{Bn*}$ and their derivatives is outlined in Scheme 1. All new compounds except $\mathbf{1}^{Bn}$ have been structurally characterised by single-crystal X-ray diffraction (XRD; vide infra). Like all known fcNHCs $\mathbf{1}^{R}$, the target carbenes were accessed by deprotonation of corresponding formamidinium salts ($\mathbf{1}^{R}H[BF_4]$), which were synthesised from 1,1′-diaminoferrocene derivatives of the type $fc(NHR)_2$ and triethyl orthoformate in the presence of $NH_4[BF_4]$.[11] The sequence starts from 1,1′-diaminoferrocene (**2**), which is subjected to a condensation reaction with PhCHO or MesCHO to furnish the imines fc(N=CHPh) (**3a**) and fc(N=CHMes) (**3b**), which are subsequently transformed to the diamines $fc(NHBn)_2$ (**4a**) and $fc(NHBn^*)_2$ (**4b**) by reduction with $Li[AlH_4]$. **3a** and **4a** are known compounds, which were reported already more than two decades ago by Gibson and Long.[12] The new diaminoferrocene **4b** was obtained in an excellent yield of 84% with respect to 1,1′-diaminoferrocene (**2**) by a one-pot procedure; for comparison, a yield of 38% over two steps was achieved by Gibson and Long for **4a**.

The molecular structures of **3b** and **4b** are shown in Figure 2 and Figure 3, respectively.

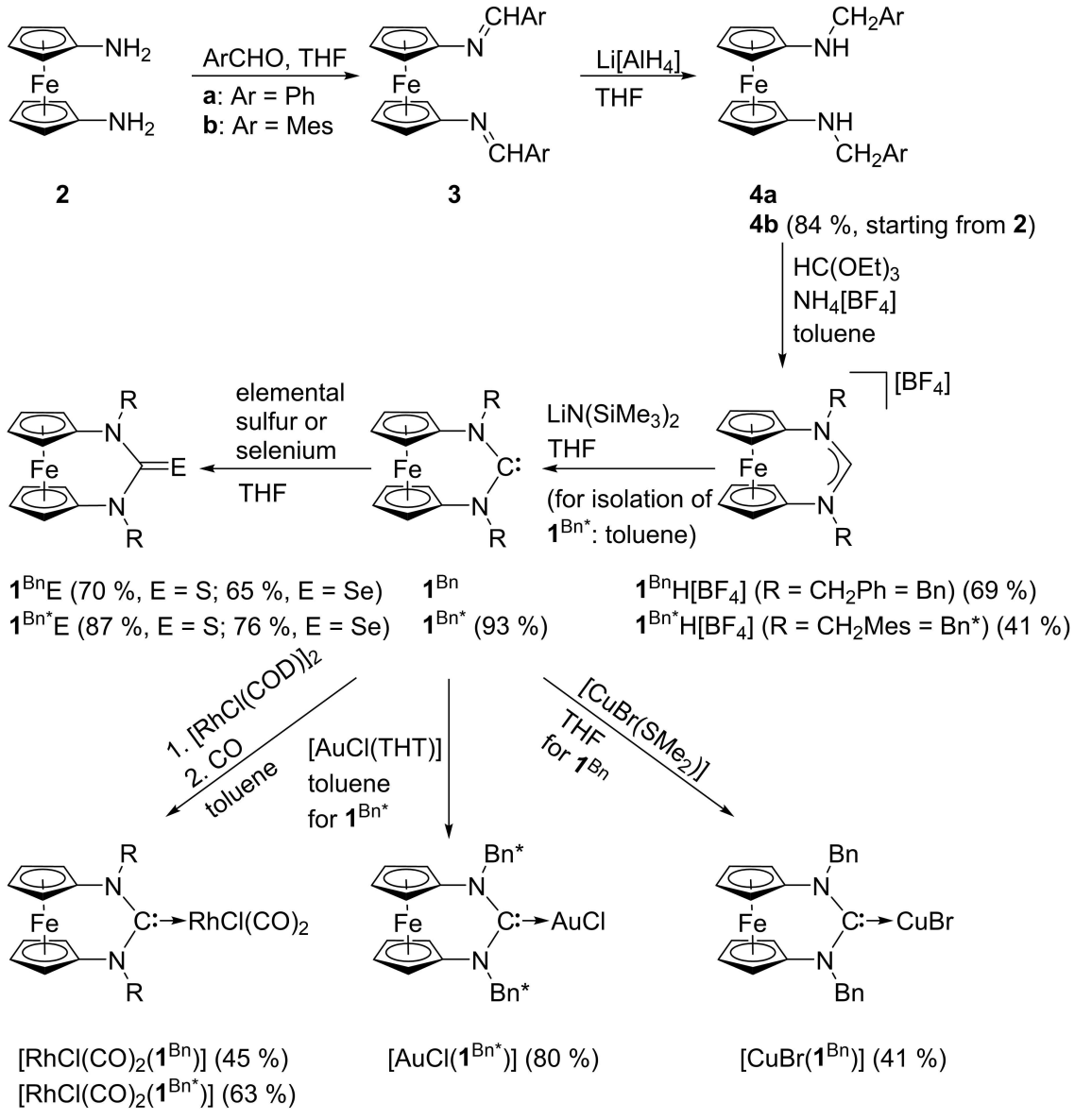

Scheme 1. Synthesis of the target fcNHCs $\mathbf{1}^{Bn}$ and $\mathbf{1}^{Bn*}$ and their derivatives investigated in this study (COD = cycloocta-1,5-diene, THT = tetrahydrothiophene). Isolated yields for new compounds are given in brackets.

 © 2022 The Authors. Zeitschrift für anorganische und allgemeine Chemie published by Wiley-VCH GmbH

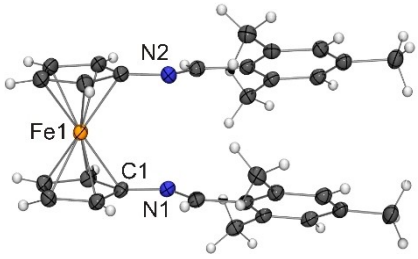

Figure 2. Molecular structure of **3 b** in the crystal (ORTEP with 30 % probability ellipsoids).

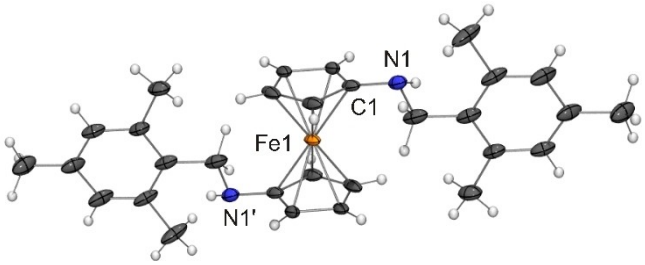

Figure 3. Molecular structure of **4 b** in the crystal (ORTEP with 30 % probability ellipsoids).

The structural features of diimine **3 b** are similar to those of fc(NH=CH–*p*-C_6H_4–OMe)$_2$.[10] The N_{imine} atoms of **3 b** each exhibit two significantly different C–N bond lengths, on average ca. 1.41 and 1.28 Å, respectively, which is in accord with a single and a double bond between sp^2-hybridised carbon and nitrogen atoms. The cyclopentadienyl rings are essentially coplanar (tilt angle 2.7°) and adopt a staggered conformation (torsion angle N–C_{ipso}–C_{ipso}–N 24.8°). The molecule has an approximate non-crystallographic C_2 symmetry about an axis that passes through the Fe atom and bisects the vector linking the two N atoms. The dihedral angles between the best planes of the mesityl rings and their respective cyclopentadienyl ring are 31.4° and 31.2°, which is substantially larger than the values found for fc(NH=CH–*p*-C_6H_4–OMe)$_2$ (8.5° and 11.8° for molecule 1, 12.1° and 16.8° for molecule 2), thus indicating intramolecular steric repulsion due to *o*-Me groups.

The molecular structure of diamine **4 b** closely resembles that of fc(NH=CH–*p*-C_6H_4–NMe_2)$_2$,[10] exhibiting crystallographically imposed inversion symmetry (molecular point group C_i), which is reflected in a fully staggered orientation of the cyclopentadienyl rings with diametrically opposed amino substituents. The C–N bond lengths of 1.397(6) and 1.462(6) Å are in accord with single bonds between an sp^3-hybridised nitrogen atom and sp^2- and sp^3-hybridised carbon atoms, respectively.

The formylative cyclisation of **4 a** and **4 b** afforded the immediate carbene precursors **1**^{Bn}H[BF_4] and **1**^{Bn*}H[BF_4] in yields of 69 % and 41 %, respectively. The molecular structures are shown in Figure 4 and Figure 5. Pertinent interatomic distances and angles of these and all other new [3]ferrocenophane-type compounds of this study are collected in Table 1.

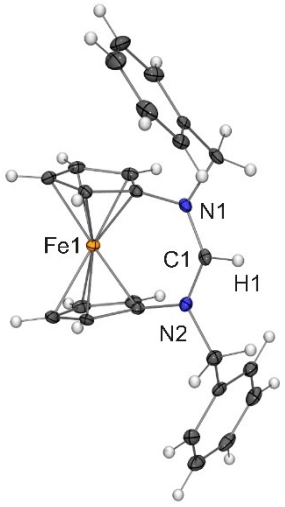

Figure 4. Molecular structure of the cation of **1**^{Bn}H[BF_4] in the crystal (ORTEP with 30 % probability ellipsoids).

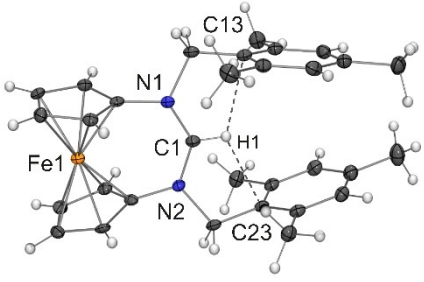

Figure 5. Molecular structure of the cation of **1**^{Bn*}H[BF_4]·THF in the crystal (ORTEP with 30 % probability ellipsoids, solvent molecule omitted for clarity). Short N_2CH···C_{arene} contacts (2.33 Å, C–H–C ca. 110°) are indicated by dashed lines.

The two formamidinium cations share a number of characteristic structural features. The bonding environment of the N atoms is trigonal planar in each case. The N–C–N angle is ca. 129° and the C–N bond lengths in this unit are ca. 1.32 Å. Due to the presence of the triatomic bridge, the cyclopentadienyl rings are substantially tilted by ca. 16° and adopt an essentially eclipsed orientation (twist angles $\leq$6.2°). These values are in line with those of other ferrocene-based formamidinium cations.[1,7] The cation of **1**^{Bn}H[BF_4] exhibits approximate non-crystallographic C_2 symmetry along an axis that passes through the Fe atom and the formamidinium C atom. The phenyl groups are leaning towards the fc moiety, but are located on opposite sides. They are in a fly-trap like arrangement with the cyclopentadienyl ring they are connected to by a CH_2 unit, forming a dihedral angle of ca. 45° and 57°, respectively. In contrast, the mesityl rings of **1**^{Bn*}H[BF_4] are pointing away from the fc moiety and in the same direction, the corresponding dihedral angles being only ca. 5° and 11°. The hydrogen atom of the cationic N_2CH unit exhibits short contacts to the CH_2-bonded C atom of each mesityl group (Figure 5), compatible with weak CH···π(ar-

 © 2022 The Authors. Zeitschrift für anorganische und allgemeine Chemie published by Wiley-VCH GmbH

Table 1. Pertinent interatomic distances/Å and angles/° of the new [3]ferrocenophane-type compounds of this study.

	N–C[a]	N–C–N	C–E[a]	Tilt angle[b]	Twist angle[c]	CH···E contacts
$1^{Bn}H[BF_4]$	1.317(4)	129.3(3)		16.0	1.5	
	1.319(4)					
$1^{Bn*}H[BF_4]$	1.319(5)	129.3(4)		16.5	6.2	
	1.317(5)					
$1^{Bn*}HCl$[d]	1.312(10)	129.1(8)		16.2	0.1	
	1.319(10)	129.5(8)		15.4	2.6	
	1.307(10)					
	1.340(10)					
1^{Bn*}	1.358(3)	119.0(2)		16.7	9.5	
	1.356(3)					
$1^{Bn}S$	1.363(3)	120.9(3)	1.696(4)[e]	18.6	11.2	2.45[e]
	1.363(3)					2.45[e]
$1^{Bn*}S$	1.362(3)	121.2(2)	1.698(2)[e]	18.8	2.8	2.45[e]
	1.368(3)					2.45[e]
$1^{Bn}Se$[d]	1.358(7)	120.8(4)	1.852(5)[f]	18.4	12.0	2.60[f]
	1.382(7)	120.0(4)	1.849(5)[f]	19.7	19.6	2.56[f]
	1.373(6)					2.57[f]
	1.374(6)					2.60[f]
$1^{Bn*}Se$	1.366(3)	121.7(2)	1.870(2)[f]	19.0	2.5	2.52[f]
	1.357(3)					2.52[f]
cis-$[RhCl(CO)_2(1^{Bn})]$	1.358(6)	122.9(4)	2.112(5)[g]	16.8	3.6	2.47[g]
	1.336(6)					2.45[g]
cis-$[RhCl(CO)_2(1^{Bn*})]$	1.347(3)	122.5(2)	2.091(2)[g]	17.6	7.3	2.51[g]
	1.349(3)					2.61[g]
$[AuCl(1^{Bn*})]$[d]	1.353(6)	122.5(4)	2.012(5)[h]	17.9	2.3	
	1.343(7)	122.4(4)	2.015(5)[h]	18.5	0.7	
	1.345(6)					
	1.355(6)					
$[CuBr(1^{Bn})]$	1.349(3)	122.3(2)	1.923(2)[i]	16.1	4.3	
	1.348(3)					

a) Refers to the N_2C unit. b) Dihedral angle formed by the best planes of the cyclopentadienyl rings. c) N–C_{ipso}–C_{ipso}–N torsion angle. d) Two independent molecules. e) E = S. f) E = Se. g) E = Rh. h) E = Au. i) E = Cu.

ene) interactions.[13] The N_2CH moiety gives rise to a fairly broad low-field signal in the ^{1}H NMR spectrum ($CDCl_3$) at $\delta = 9.04$ and 7.91 ppm for $1^{Bn}H[BF_4]$ and $1^{Bn*}H[BF_4]$, respectively. The substantial chemical shift difference ($\Delta\delta = 1.13$ ppm) is plausibly due to the presence of CH···π(arene) interactions in the case of $1^{Bn*}H[BF_4]$ also in chloroform solution. The corresponding signal of the chloride $1^{Bn*}HCl$ (synthesised from 1^{Bn*} and Et_3NHCl; not shown in Scheme 1) is observed at $\delta = 9.77$ ppm, down-field shifted by 1.86 ppm with respect to $1^{Bn*}H[BF_4]$. It is well known for formamidinium salts that chloride anions can lead to down-field shifts of the N_2CH ^{1}H NMR signal of ca. 2 ppm in $CDCl_3$ with respect to the weakly coordinating anion $[BF_4]^-$, which may be ascribed to comparatively strong N_2CH···Cl hydrogen bond interactions.[14] Not surprisingly, such a hydrogen bond is evident from the molecular structure of $1^{Bn*}HCl$ in the solid state (Figure 6; average values for the two independent molecules present in the asymmetric unit: CH···Cl 2.45 Å, C–H–Cl 172°). The metric parameters of the N_2C unit are essentially identical to those of $1^{Bn}H[BF_4]$ and $1^{Bn*}H[BF_4]$, indicating that the degree of π-delocalisation in this unit is substantially higher for the formamidinium cations than for the other compounds collected in Table 1, which invariably exhibit longer C–N bonds and more acute N–C–N angles. Similar to $1^{Bn*}H[BF_4]$, the mesityl rings of

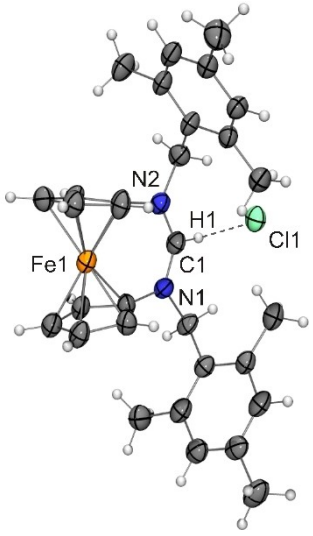

Figure 6. Molecular structure of $1^{Bn*}HCl$ in the crystal (ORTEP with 20 % probability ellipsoids). The CH···Cl hydrogen bond is indicated by a dashed line.

 © 2022 The Authors. Zeitschrift für anorganische und allgemeine Chemie published by Wiley-VCH GmbH

$\mathbf{1}^{Bn*}$HCl are located on the same side of the fc unit. However, their relative orientation with respect to the corresponding cyclopentadienyl ring resembles that of the phenyl rings of $\mathbf{1}^{Bn}$H[BF_4], the dihedral angles formed with the respective cyclopentadienyl ring being 50.7 and 51.6° for molecule 1 and 66.8 and 51.2° for molecule 2.

The target fcNHCs $\mathbf{1}^{Bn}$ and $\mathbf{1}^{Bn*}$ were generated by treatment of the corresponding precursor with LiN($SiMe_3$)$_2$ in toluene or THF. $\mathbf{1}^{Bn}$ was too unstable for direct observation even at low temperatures, but could be efficiently trapped with elemental sulfur or selenium. In contrast, $\mathbf{1}^{Bn*}$ was isolated as a thermally stable crystalline solid in 93% yield. The molecular structure is shown in Figure 7.

Similar to its formamidinium precursors $\mathbf{1}^{Bn*}$HX (X = [BF_4], Cl), the cyclopentadienyl rings of $\mathbf{1}^{Bn*}$ are tilted by ca. 17° and adopt an essentially eclipsed orientation (twist angle 9.5°). The carbene bond angle of $\mathbf{1}^{Bn*}$ is 119.0(2)° and the $C_{carbene}$–N bond lengths are ca. 1.36 Å, which corresponds to a substantial narrowing of the N–C–N angle by 10° and a significant lengthening (by 0.04 Å) of the bonds in the N_2C unit with respect to the formamidinium precursors. This is in line with our previous observations in this chemistry and, as mentioned above, indicates a comparatively lower degree of π-delocalisation in the N_2C unit of the carbene,[7] as already noted by Arduengo in his seminal paper describing the first stable diaminocarbene.[15] The mesityl rings of $\mathbf{1}^{Bn*}$ are leaning towards the fc moiety similar to their orientation in $\mathbf{1}^{Bn*}$HCl, forming a dihedral angle of 58° and 59°, respectively, with their respective cyclopentadienyl ring. The $C_{carbene}$ atom of $\mathbf{1}^{Bn*}$ gives rise to a ^{13}C NMR signal at δ = 259.3 ppm in C_6D_6 solution, which is close to the values reported for the few other stable fcNHCs, which lie in the narrow range from 268.1 (R = neopentyl) to 260.7 ppm (R = 2-adamantyl).[7] For comparison, conventional Arduengo carbenes based on the five-membered heterocycles imidazole, imidazoline or 1,2,4-triazole exhibit corresponding signals between ca. 210 and 245 ppm and even six-membered congeners do not exhibit signals downfield from 245 ppm in C_6D_6.[16] The carbene bond angles of five-membered Arduengo carbenes typically lie in the range from 100–106°,[4] whereas six-membered congeners have considerably larger carbene bond angles of ca. 115°.[17] As already noted above, fcNHCs $\mathbf{1}^{R}$ can be regarded as six-membered NHCs, which, however, contain a comparatively large atom, Fe, in the heterocycle (Figure 1). Consequently, their carbene bond angles (ca. 120°)[7] are larger than those of conventional six-membered NHCs and very similar to those of acyclic diaminocarbenes (ADACs);[5] an analogous similarity can be noted for the chemical shift range of the ^{13}C NMR signal of the $C_{carbene}$ atom of ADACs and fcNHCs $\mathbf{1}^{R}$ (ca. 259–268 ppm, vide supra).[5a,b,16,18] The correlation of the $C_{carbene}$ bond angle and the chemical shift of its ^{13}C NMR signal is well known and was described for cyclic diaminocarbenes already in 2006 by Kunz.[19] The $C_{carbene}$ bond angle is related both to the σ-donor strength and to the electrophilicity of a singlet carbene. A widening of this angle increases the p-character, and hence energy, of the carbene HOMO, causing an increase in σ-donicity and nucleophilicity.[20] In turn, the increase in HOMO energy causes a decrease of the HOMO–LUMO gap, which correlates with the singlet–triplet energy separation (ΔE_{ST}),[21] and a low ΔE_{ST} value indicates a high electrophilicity of a singlet carbene.[8a,22] A simple method for estimating the σ-donor strength of carbenes is the analysis of the $^1J_{CH}$ coupling constants of their protonated forms, viz. the corresponding formamidinium cations.[23] $^1J_{CH}$ values >200 Hz have been reported for conventional five- and six-membered NHCs.[24] The $^1J_{CH}$ values determined for $\mathbf{1}^{Bn}$H[BF_4] and $\mathbf{1}^{Bn*}$H[BF_4] from proton-coupled ^{13}C NMR spectra[25] in $CDCl_3$ solution are 190 and 191 Hz, respectively, indicating a σ-donor strength of the fcNHCs substantially higher than that of conventional NHCs and similar to that of CAACs.[26] $\mathbf{1}^{Bn*}$HCl exhibits a significantly larger $^1J_{CH}$ value of 196 Hz, which is plausibly related to the N_2CH···Cl hydrogen bond interactions already discussed above for this compound.[27] The electrophilicity of the fcNHCs $\mathbf{1}^{Bn}$ and $\mathbf{1}^{Bn*}$ was probed by a ^{77}Se NMR spectroscopic investigation of the corresponding selenourea derivatives $\mathbf{1}^{Bn}$Se and $\mathbf{1}^{Bn*}$Se. This convenient method was developed by Ganter,[28] whose work was subsequently extended by Nolan, confirming that $\delta(^{77}Se)$ values of carbene–selenium adducts can be deployed with confidence to quantify the π-accepting capability of the parent carbenes.[29] The selenourea derivatives were readily prepared by reacting grey selenium with $\mathbf{1}^{Bn}$ and $\mathbf{1}^{Bn*}$, respectively (Scheme 1); for this purpose the carbenes were generated in situ from $\mathbf{1}^{R}$[BF_4] (R = Bn, Bn*) and LiN($SiMe_3$)$_2$ in THF. $\mathbf{1}^{Bn}$Se and $\mathbf{1}^{Bn*}$Se exhibit $\delta(^{77}Se)$ values of 321 and 359 ppm, respectively, in acetone-d_6 solution, which is close to the values of the previously reported *N*-benzylic congeners (323 and 318 ppm for R = CH_2–*p*-C_6H_4–OMe and CH_2–*p*-C_6H_4–NMe_2, respectively;[10] experimental values obtained in $CDCl_3$ and converted to acetone-d_6 by using a published correlation).[5b] The ^{77}Se NMR signals of these fcNHC–selenium adducts are substantially down-field shifted with respect to the range of ca. 0–200 ppm reported for selenium adducts of conventional

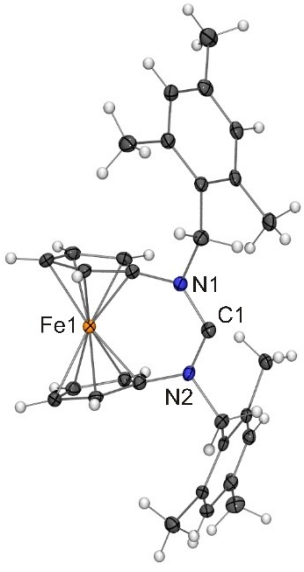

Figure 7. Molecular structure of $\mathbf{1}^{Bn*}$ in the crystal (ORTEP with 30% probability ellipsoids).

 © 2022 The Authors. Zeitschrift für anorganische und allgemeine Chemie published by Wiley-VCH GmbH

NHCs.[29] For comparison, ADAC–selenium adducts show even more down-field-shifted signals with $\delta(^{77}Se) > 400$ ppm in acetone-d_6.[5b] Despite the rather similar $C_{carbene}$ bond angles of ADACs and fcNHCs, the higher π-accepting capability of ADACs is plausible because the higher conformational flexibility of the acyclic framework leads to a reduced degree of π-stabilisation of the divalent carbon atom by the lone pairs of the flanking nitrogen atoms. With $\delta(^{77}Se) > 480$ ppm in acetone-d_6,[30] CAACs are also more electrophilic than fcNHCs on the ^{77}Se NMR scale, which can be ascribed to the π-stabilisation of the $C_{carbene}$ atom by only a single nitrogen atom. As a caveat we note that the reliability of the ^{77}Se NMR scale may be compromised by intramolecular C(sp^3)H···Se interactions, which have been observed in the structures of selenium adducts of carbenes with particularly bulky *N*-substituents and may cause a significant down-field shift of the ^{77}Se NMR signal, thus triggering a non-linear behaviour of this NMR spectroscopic scale.[30] The molecular structures of **1**^{Bn}Se (Figure 8) and **1**^{Bn*}Se (Figure 9) indeed exhibit contacts between the selenium atom and a hydrogen atom of each CH_2 moiety between ca. 2.52 and 2.60 Å, which already fall in the range where a significant influence on the ^{77}Se chemical shift may be expected.

The C–Se bond lengths are 1.852(5) and 1.849(5) Å for the two independent molecules of **1**^{Bn}Se and 1.870(2)Å for **1**^{Bn*}Se. These values are very similar to those of the previously reported *N*-benzylic congeners **1**^{R}Se, viz. 1.857(6) and 1.843(4) Å for R = CH_2–*p*-C_6H_4–OMe and CH_2–*p*-C_6H_4–NMe_2, respectively[10] and compare well with the C–Se bond lengths of imidazole- and imidazoline-based selenourea derivatives, which typically lie in the range from ca. 1.82 to 1.86 Å.[23a,29,32,33] Selenium adducts of ADACs and CAACs exhibit values at the lower end of this range,[5a,b,30,34] in accord with the high electrophilicity of these carbenes. The thiourea derivatives **1**^{Bn}S (Figure 10) and **1**^{Bn*}S (Figure 11), which were obtained analogously from **1**^{Bn} and **1**^{Bn*} and elemental sulfur (Scheme 1), have C–S bond lengths of 1.696(4) and 1.698(2) Å. These values are in concert with the C–Se bond lengths discussed above in view of the 0.15 Å difference of the covalent radii of S (1.05 Å) and Se (1.20 Å).[36] A very similar C–S bond length of 1.685(3) Å has been determined for the *tert*-butyl homologue **1**^{tBu}S.[7a] In comparison to the C–E distances (E = S, Se) of thioketones (ca. 1.62 Å)[37] and selenoketones (ca. 1.77 Å),[38] the corresponding distances of **1**^{Bn}E and **1**^{Bn*}E are substantially longer (by ca. 0.08 Å). Such elongated bonds are typical for cyclic thio- or selenoureas, in line with a significant contribution of zwitterionic canonical structures N_2C^+–E^- featuring single dative bonds,[39,40] which are plausibly beneficial for intramolecular C(sp^3)H···E interactions indicated by

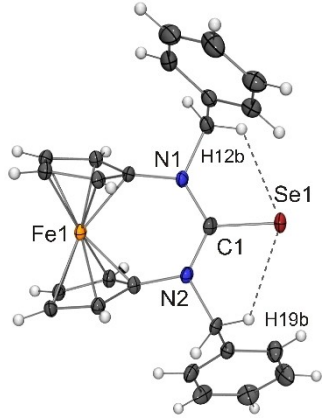

Figure 8. Molecular structure of **1**^{Bn}Se in the crystal (ORTEP with 30 % probability ellipsoids). C(sp^3)H···Se contacts are indicated by dashed lines (C–H–Se ca. 110 and 114°).[31]

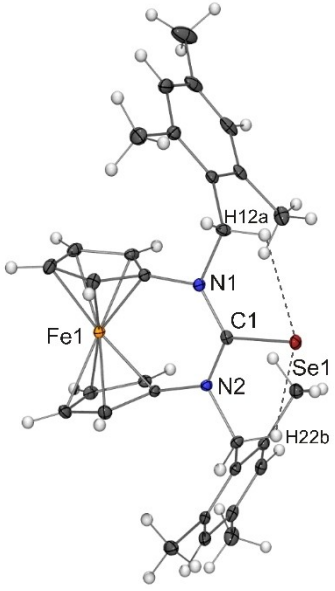

Figure 9. Molecular structure of **1**^{Bn*}Se in the crystal (ORTEP with 30 % probability ellipsoids). C(sp^3)H···Se contacts are indicated by dashed lines (C–H–Se ca. 114 and 116°).[31]

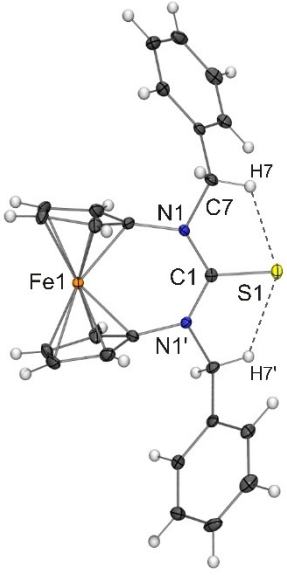

Figure 10. Molecular structure of **1**^{Bn}S in the crystal (ORTEP with 30 % probability ellipsoids). C(sp^3)H···S contacts are indicated by dashed lines (C–H–S ca. 115°).[35]

 © 2022 The Authors. Zeitschrift für anorganische und allgemeine Chemie published by Wiley-VCH GmbH

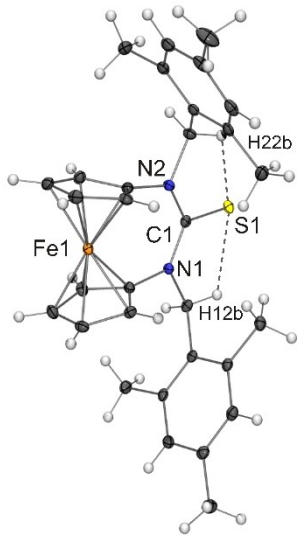

Figure 11. Molecular structure of $\mathbf{1}^{Bn*}S$ in the crystal (ORTEP with 30% probability ellipsoids). C(sp^3)H···S contacts are indicated by dashed lines (C–H–S ca. 112 and 113°).[35]

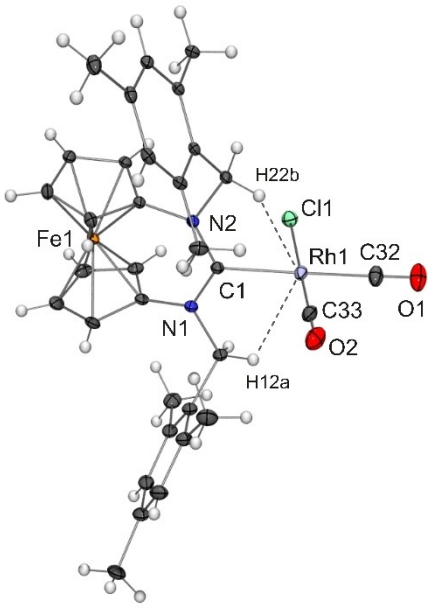

Figure 12. Molecular structure of *cis*-[RhCl(CO)$_2$($\mathbf{1}^{Bn*}$)] in the crystal (ORTEP with 30% probability ellipsoids). C–H···Rh contacts compatible with anagostic interactions are indicated by dashed lines (C–H–Rh ca. 116 and 119°). Selected bond lengths/Å and angles/°: Rh1–Cl1 2.3466(8), Rh1–C32 1.914(3), Rh1–C33 1.871(3), O1–C32 1.101(4), O2–C33 1.108(4); C1–Rh1–Cl1 82.60(7), C32–Rh1–Cl1 89.51(11), C32–Rh1–C1 171.12(12), C33–Rh1–Cl1 175.73(9), C33–Rh1–C1 96.63(12), C33–Rh1–C32 91.53(14), O1–C32–Rh1 177.0(3), O2–C33–Rh1 179.4(3).

the rather short contacts (on average ca. 2.45 and 2.56 Å for E = S and Se, respectively; see Table 1 and Figures 8–11) present in these compounds.

The NMR spectroscopic data of $\mathbf{1}^{Bn*}$ and its proton and selenium adducts indicate that this carbene is substantially more nucleophilic and more electrophilic than Arduengo carbenes, exhibiting an ambiphilicity already similar to that of CAACs. This notion is supported by the averaged carbonyl stretching frequency $\tilde{\nu}_{av}$(CO) = 2038 cm^{-1} of the Rh^{I} complex *cis*-[RhCl(CO)$_2$($\mathbf{1}^{Bn*}$)] (Scheme 1) in CH_2Cl_2 solution,[24,41] which is very similar to that of conventional CAAC analogues *cis*-[RhCl(CO)$_2$(CAAC)] (a value of 2037 cm^{-1} has been determined for the simplest stable CAAC).[42] The molecular structure of *cis*-[RhCl(CO)$_2$($\mathbf{1}^{Bn*}$)] is shown in Figure 12.

The Rh^{I} atom is in the square-planar coordination environment typical of tetracoordinate d^8 metal complexes. The Rh–$C_{carbene}$ distance is 2.091(2) Å, which compares well with the bond lengths of other congeners of the type [RhCl(CO)$_2$($\mathbf{1}^{R}$)] and of closely related complexes.[1c,7c] The Rh–CO distances are significantly different, viz. 1.914(3) and 1.871(3) Å for the CO ligand positioned *trans* and *cis*, respectively, to the coordinated fcNHC, which is in line with the pronounced *trans* influence[43] of NHC ligands.[44] One hydrogen atom of each CH_2 unit is engaged in a short C–H···Rh contact (2.51 and 2.61 Å, indicated by dashed lines in Figure 12), compatible with intramolecular anagostic interactions.[45] Low-field shifts of 1 ppm or more are typically observed for ^{1}H NMR signals of protons involved in anagostic interactions.[45b,c,46] While a singlet at δ = 5.34 ppm is observed for the CH_2 protons of $\mathbf{1}^{Bn*}$ in C_6D_6 solution, the CH_2 protons of *cis*-[RhCl(CO)$_2$($\mathbf{1}^{Bn*}$)] are diastereotopic, giving rise to two doublets ($^2J_{HH}$ = 13.6 Hz) in the ^{1}H NMR spectrum at δ = 6.28 and 5.19 ppm in $CDCl_3$. The low-field shift of only one of the signals due to the diastereotopic CH_2 protons is in concert with the observation that only one of the hydrogen atoms of each CH_2 unit is engaged in a short C–H···Rh contact. The analogous complex containing $\mathbf{1}^{Bn}$ exhibits rather similar structural (Figure 13) and spectroscopic features. In comparison, its averaged carbonyl stretching frequency $\tilde{\nu}_{av}$(CO) = 2041 cm^{-1} (CH_2Cl_2) is slightly blue-shifted (by 3 cm^{-1}). The CH_2 protons of *cis*-[RhCl(CO)$_2$($\mathbf{1}^{Bn}$)] give rise to two doublets in the ^{1}H NMR spectrum at δ = 6.50 and 5.36 ppm in $CDCl_3$, exhibiting a slightly higher $\Delta\delta$ value (1.14 vs. 1.09 ppm) and $^2J_{HH}$ coupling constant (14.5 vs. 13.6 Hz) than *cis*-[RhCl(CO)$_2$($\mathbf{1}^{Bn*}$)]. In line with this, the C–H···Rh contacts in *cis*-[RhCl(CO)$_2$($\mathbf{1}^{Bn}$)] are ca. 2.45 and 2.47 Å and thus slightly shorter (by 0.1 Å on average) than those in *cis*-[RhCl(CO)$_2$($\mathbf{1}^{Bn*}$)].

A comparison of this pair of complexes reveals that, like in the free carbene $\mathbf{1}^{Bn*}$, the mesityl groups are positioned on the same side of the fc unit, whereas the phenyl groups are located on opposite sides. The same holds true for the sulfur and selenium adduct pairs. Interestingly, the gold(I) complex [AuCl($\mathbf{1}^{Bn*}$)] (Scheme 1), which was synthesised primarily to analyse the steric demand of $\mathbf{1}^{Bn*}$ by determining its percent buried volume (%V_{bur}),[47] contains two independent molecules in the asymmetric unit (Figure 14), which differ in the orientation of the Mes groups, namely positioned either on the same side (molecule 1) or on different sides of the fc unit (molecule 2). This results in distinctly different steric maps and also has a substantial influence on the %V_{bur} value calculated for an assumed Au–C distance of 2.00 Å (Figure 14), which is

 © 2022 The Authors. Zeitschrift für anorganische und allgemeine Chemie published by Wiley-VCH GmbH

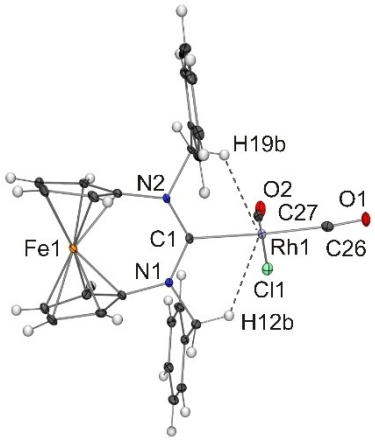

Figure 13. Molecular structure of *cis*-[RhCl(CO)$_2$(**1**^{Bn})] in the crystal (ORTEP with 30% probability ellipsoids). C–H···Rh contacts compatible with anagostic interactions are indicated by dashed lines (C–H–Rh ca. 126 and 127°). Selected bond lengths/Å and angles/°: Rh1–Cl1 2.3522(12), Rh1–C26 1.911(6), Rh1–C27 1.845(6), O1–C26 1.131(7), O2–C27 1.140(7); C1–Rh1–Cl1 85.15(13), C26–Rh1–Cl1 91.43(16), C26–Rh1–C1 174.3(2), C27–Rh1–Cl1 172.8(2), C27–Rh1–C1 95.0(2), C27–Rh1–C26 88.9(2), O1–C26–Rh1 176.0(5), O2–C27–Rh1 171.6(5).

35.8% in molecule 1 and 38.0% in molecule 2 ($\Delta\%V_{bur} = 2.2\%$), close to the values of 36.5 and 36.9% reported for the standard five-membered NHCs IMes and SIMes, respectively,[47c] and intermediate between the values of 33.5 and 42.2% determined from corresponding gold(I) complexes for six-membered NHCs with benzyl and mesityl *N*-substituents, respectively.[6a,48] NHCs can undergo conformational changes in response to their coordination environment, and the flexibility of their $\%V_{bur}$ is important for chemical reactions at the metal centre.[49,50] For example, a $\%V_{bur}$ range from 30–34% has been calculated for SIMes in the "Grubbs II initiator" model complex [RuCl$_2$(=CH$_2$)(PMe$_3$)(SIMes)] in this context.[49] Different conformations of [AuCl(NHC)] in the solid state affording different $\%V_{bur}$ values are not unprecedented, but have not resulted in substantial differences so far ($\Delta\%V_{bur}$ 0.5%).[51] The copper(I) complex [CuBr(**1**^{Bn})] (Scheme 1) was used for calculating the $\%V_{bur}$ value of the unstable fcNHC **1**^{Bn}, because all attempts to synthesise [AuCl(**1**^{Bn})] afforded only intractable material. Note that the $\%V_{bur}$ values obtained for NHCs from quasilinear dicoordinate copper(I) and gold(I) complexes differ only marginally, when the same M–C distance of 2.00 Å is assumed.[47c] The molecular structure of [CuBr(**1**^{Bn})] (Figure 15) resembles that of molecule 2 in the asymmetric unit of [AuCl(**1**^{Bn*})], since the aryl groups are positioned on different sides of the fc unit in each case. The $\%V_{bur}$ of **1**^{Bn} (34.9%) is lower than that of **1**^{Bn*} (38.0% for molecule 2), in line with the lower steric demand of Ph vs. Mes.

Conclusion

We have studied the new stable fcNHC fc[(NCH$_2$Mes)$_2$C:] (**1**^{Bn*}). Its $\%V_{bur}$ value is similar to that of the popular Arduengo carbenes IMes and SIMes, pointing to a moderate steric demand. NMR and IR spectroscopic data indicate a pronounced ambiphilicity of this carbene untypical of Arduengo carbenes or related cyclic diaminocarbenes and already similar to that of CAACs, which can be ascribed to the large $C_{carbene}$ bond angle of 119° determined for **1**^{Bn*} by XRD. Being too unstable for direct experimental observation even at low temperatures, the sterically less protected homologue fc[(NCH$_2$Ph)$_2$C:] (**1**^{Bn}) was characterised through trapping reactions. In terms of its thermal stability, fc[(NCH$_2$Mes)$_2$C:] (**1**^{Bn*}) is strongly reminiscent of the neopentyl homologue fc[(NCH$_2$*t*Bu)$_2$C:], which may be related to a similar steric impact of *t*Bu and Mes vicinal to the $C_{carbene}$ atom.[52] In view of the presence of numerous benzylic, and therefore activated, C(sp^3)–H bonds in **1**^{Bn*}, a decomposition of this fcNHC by insertion of its divalent carbon atom into such a bond could have been expected. Such an insertion has been observed at 70 °C for a six-membered NHC with *N*-mesityl substituents[53] and already at room temperature for an *N*-mesityl substituted CAAC with a 1,1′-ferrocenylene backbone.[26a] We surmise that the comparatively higher flexibility due to the CH$_2$ unit between the mesityl group and the N atom in **1**^{Bn*} has a protective influence in this context, lowering the degree of preorganisation for the insertion reaction. The behaviour of fcNHC **1**^{Bn*} suggests that homologues with similar benzylic substituents such as, for example, CH$_2$–C$_6$H$_2$–2,4,6-(CF$_3$)$_3$ or CH$_2$–C$_6$H$_3$–3,5-Me$_2$ may be sufficiently stable for isolation, too. Such fcNHCs will be investigated in terms of small-molecule activation chemistry. It is well known from the closely related chemistry of CAACs in this context that small changes in the substituents close to the $C_{carbene}$ atom may have a large influence on the reactivity of the carbene.[42,54]

Experimental Section

All reactions involving air-sensitive compounds were performed in an inert atmosphere (argon or dinitrogen) by using Schlenk techniques or a conventional glovebox. Starting materials were procured from standard commercial sources and used as received. 1,1′-Diaminoferrocene (**2**), 1,1′-di(benzylamino)ferrocene (**4a**) and [AuCl(THT)] were synthesised by following adapted versions of the published procedures.[12,55,56] NMR spectra were recorded at ambient temperature with Varian NMRS-500 and MR-400 spectrometers operating at 500 and 400 MHz, respectively, for ^{1}H. ^{77}Se NMR spectra were recorded with a Varian NRMS-500 spectrometer with neat dimethylselenide as external standard ($\delta = 4$ ppm).[57] IR spectra were obtained with a Bruker ALPHA FT-IR spectrometer. Combustion analyses were carried out with a HEKAtech Euro EA-CHNS elemental analyser at the Institute of Chemistry, University of Kassel, Germany.

Synthesis of fc(NHBn*)$_2$ (4b): A solution of 1,1′-diaminoferrocene (**2**; 2.61 g, 12.1 mmol) and 2,4,6-trimethylbenzaldehyde (3.58 g, 24.2 mmol) in THF (50 mL) was stirred for 14 h. MgSO$_4$ (2.0 g) was added and stirring was continued for 15 min. Insoluble material was removed by filtration through a Celite pad, which was subsequently extracted with THF (2×10 mL). The imine **3b** may be isolated by standard work-up at this stage (for NMR spectra see the Supporting Information), which, however, was detrimental to the overall yield of **4b** in comparison to the one-pot procedure described in the following. The combined extracts and filtrate were

 © 2022 The Authors. Zeitschrift für anorganische und allgemeine Chemie published by Wiley-VCH GmbH

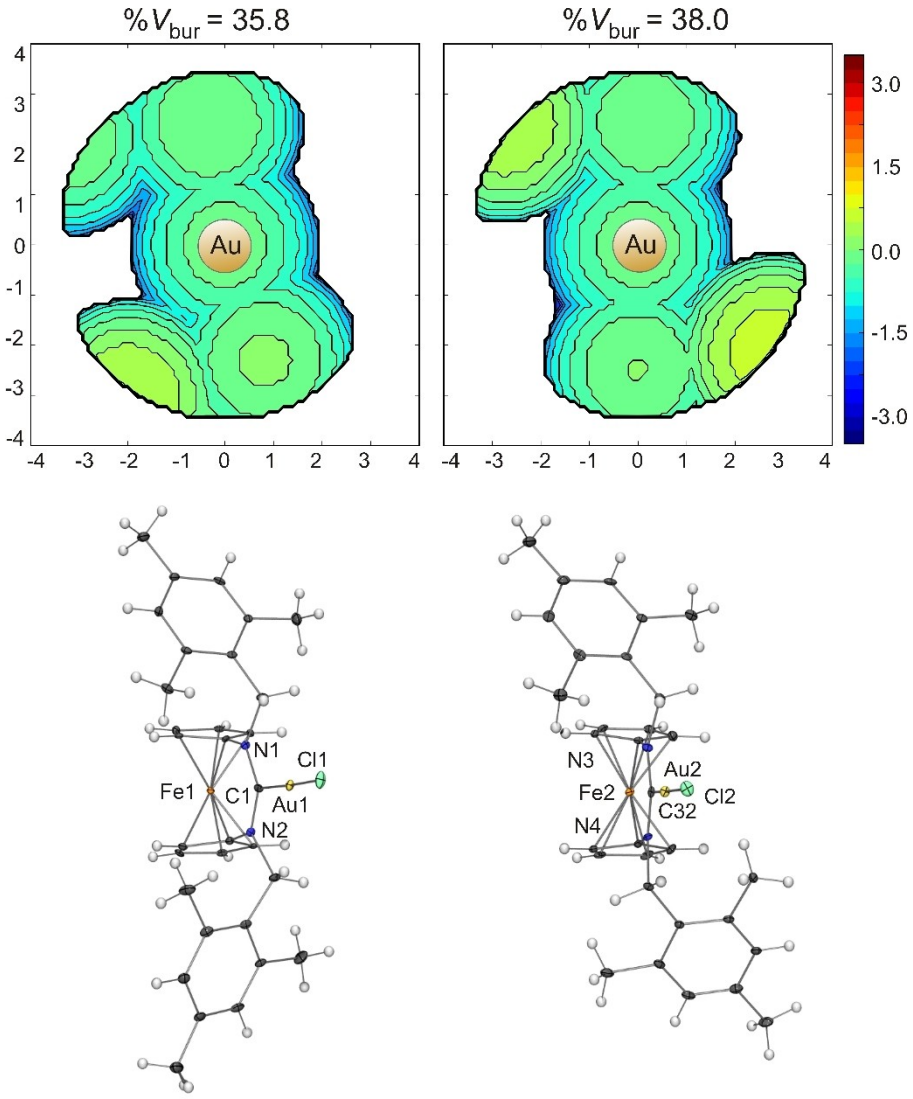

Figure 14. Molecular structures of the two independent molecules of [AuCl(1^{Bn*})] in the crystal (bottom; ORTEP with 30% probability ellipsoids), together with their steric maps calculated for an assumed Au–C distance of 2.00 Å (top). Selected bond lengths/Å and angles/°: Au1–Cl1 2.2819(13), Au2–Cl2 2.2843(13); C1–Au1–Cl1 174.71(14), C32–Au2–Cl2 176.02(14).

cooled in an ice bath. $Li[AlH_4]$ (4.13 g, 108.7 mmol) was added to the stirred solution. The cooling bath was removed after 1 h and the mixture was allowed to warm up to ambient temperature over the course of ca. 1 h. The stirred mixture was again cooled in an ice bath. Water (4.0 mL) was added dropwise. The ice bath was removed and stirring was continued for 2 h. Insoluble material was removed by filtration through a Celite pad, which was subsequently extracted with THF (4×10 mL). Volatile components were removed from the combined extracts and filtrate under vacuum, affording the product as an orange microcrystalline solid. Yield: 4.88 g (84%). **^{1}H NMR** ($CDCl_3$): δ = 6.89 (br. s, 4 H, $C_6H_2Me_3$), 4.07 (br. s, 4 H, C_5H_4), 4.02 (br. s, 8 H, C_5H_4 and CH_2), 2.42 (br. s, 12 H, *o*-Me), 2.29 (br. s, 6 H, *p*-Me), 2.20 ppm (br. s, 2 H, NH. **^{13}C{^{1}H} NMR** ($CDCl_3$): δ = 137.3, 137.1, 132.6 (3×C_{quat} Mes), 129.2 (CH Mes), 111.1 (cyclopentadienyl C_{ipso}), 63.3, 55.8 (2×cyclopentadienyl CH), 45.6 (CH_2), 21.1 (*p*-Me), 19.7 ppm (*o*-Me). $C_{30}H_{36}N_2Fe$ (480.47): calcd. C 74.99, H 7.55, N 5.83%; found: C 74.99, H 7.35, N, 5.63%.

Synthesis of 1^{Bn}H[BF_4]: Toluene (15 mL) was added to 1,1′-di(benzylamino)ferrocene (**4a**; 2.00 g, 5.05 mmol), triethyl orthoformate (1.31 g, 8.84 mmol) and $NH_4[BF_4]$ (1.48 g, 14.12 mmol) in a pressure Schlenk tube. The Schlenk tube was sealed and the mixture was stirred at an oil bath temperature of 135 °C for 3 h. The mixture was subsequently allowed to cool to ambient temperature. Insoluble material was removed by filtration through a Celite pad and was subsequently washed with toluene (3×15 mL) and finally with dichloromethane (10 mL) to extract to product. The dichloromethane extract was reduced to dryness under vacuum. The crude product was subjected to purification by column chromatography (silica gel, dichloromethane–ethyl acetate 9:1), which afforded the product as a yellow powder. Yield 1.73 g (69%). **^{1}H NMR** ($CDCl_3$): δ = 9.04 (br. s, 1 H, N_2CH), 7.26 (br. s, 10 H, Ph), 5.06 (br. s, 4 H, CH_2), 4.18 ppm (br. s, 8 H, C_5H_4). **^{13}C{^{1}H} NMR** ($CDCl_3$): δ = 161.6 (N_2C), 133.2 (C_{ipso} Ph), 130.0, 129.0, 128.9 (3×CH Ph), 91.6 (cyclopentadienyl C_{ipso}), 72.2, 68.3 (2×cyclopentadienyl CH), 63.2 ppm (CH_2). $C_{25}H_{23}N_2BF_4Fe$ (494.11): calcd. C 60.77, H 4.69, N 5.67%; found: C 60.75, H 4.78, N, 5.79%.

Synthesis of 1^{Bn*}H[BF_4]: Toluene (15 mL) was added to **4b** (4.88 g, 10.16 mmol), triethyl orthoformate (2.67 g, 18.04 mmol) and

 © 2022 The Authors. Zeitschrift für anorganische und allgemeine Chemie published by Wiley-VCH GmbH

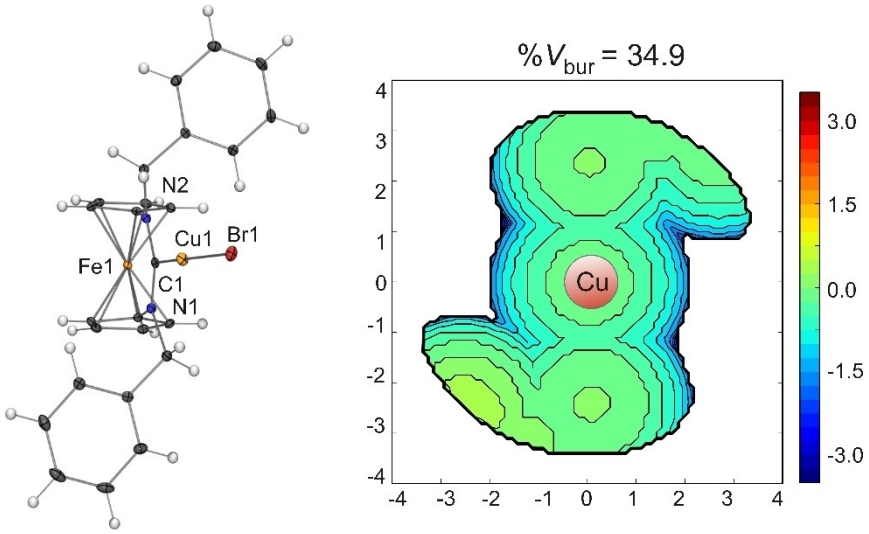

Figure 15. Molecular structure of [CuBr(**1**^{Bn})]·C_6H_6 in the crystal (left; ORTEP with 30% probability ellipsoids, solvent molecule omitted for clarity) and steric map calculated for an assumed Cu–C distance of 2.00 Å (right). Selected bond length/Å and angle/°: Br1–Cu1 2.2449(4); C1–Cu1–Br1 168.71(7).

$NH_4[BF_4]$ (3.01 g, 28.71 mmol) in a pressure Schlenk tube. The Schlenk tube was sealed and the mixture was stirred at an oil bath temperature of 130 °C for 1.5 h. The mixture was slowly cooled to −80 °C. Insoluble material was removed by filtration through a Celite pad and was subsequently washed with cold toluene (3× 15 mL) and finally at room temperature with dichloromethane (10 mL) to extract to product. The dichloromethane extract was reduced to dryness under vacuum, affording the product as a yellow microcrystalline solid. Yield 2.38 g (41%). **^{1}H NMR** ($CDCl_3$): δ = 7.91 (br. s, 1 H, N_2CH), 6.79 (br. s, 4 H, $C_6H_2Me_3$), 5.02, 4.53 (2 br. s, 2×4 H, C_5H_4), 4.30 (br. s, 4 H, CH_2), 2.26 (s, 6 H, *p*-Me), 2.20 ppm (s, 12 H, *o*-Me). **^{13}C{^{1}H} NMR** ($CDCl_3$): δ = 159.2 (N_2C), 139.0, 138.2 (2× C_{quat} Mes), 129.4 (CH Mes), 125.4 (C_{quat} Mes), 92.0 (cyclopentadienyl C_{ipso}), 72.5, 68.4 (2×cyclopentadienyl CH), 57.1 (CH_2), 21.0, 19.9 ppm (2×Me). $C_{31}H_{35}N_2BF_4Fe$ (578.27): calcd. C 64.39, H 6.10, N, 4.84%; found: C 63.84, H 6.33, N 4.56%.

Synthesis of 1^{Bn*}: Toluene (10 mL) was added to **1**^{Bn*}H[BF_4] (500 mg, 0.865 mmol) and $LiN(SiMe_3)_2$ (159 mg, 0.950 mmol). The mixture was stirred for 45 min. Insoluble material was removed by filtration through a Celite pad. The filtrate was reduced to dryness under vacuum, leaving the product as an orange microcrystalline solid. Yield 394 mg (93%). **^{1}H NMR** (C_6D_6): δ = 6.77 (s, 4 H, $C_6H_2Me_3$), 5.34 (s, 4 H, CH_2), 3.67, 3.48 (2 s, 2×4 H, C_5H_4), 2.39 (s, 12 H, *o*-Me), 2.14 ppm (s, 6 H, *p*-Me). **^{13}C{^{1}H} NMR** (C_6D_6): δ = 259.3 (N_2C), 138.9, 136.7, 132.4 (3× C_{quat} Mes), 129.4 (CH Mes), 99.6 (cyclopentadienyl C_{ipso}), 69.7, 67.7 (2×cyclopentadienyl CH), 59.2 (CH_2), 21.1 (*p*-Me), 20.9 ppm (*o*-Me).

Synthesis of 1^{Bn*}HCl: Toluene (3 mL) was added to **1**^{Bn*} (394 mg, 0.803 mmol) and Et_3NHCl (111 mg, 0.806 mmol). The mixture was stirred for 30 min and was subsequently cooled to −80 °C. The solid was removed by filtration through a Celite pad, washed with cold toluene (3×3 mL) and finally at room temperature with dichloromethane (2 mL) to extract the product. The dichloromethane extract was reduced to dryness under vacuum, affording the product as a yellow microcrystalline solid. Yield 282 mg (67%). **^{1}H NMR** ($CDCl_3$): δ = 9.77 (br. s, 1 H, N_2CH), 6.69 (s, 4 H, $C_6H_2Me_3$), 5.09 (br. s, 4 H, CH_2), 4.15, 4.05 (2 s, 2×4 H, C_5H_4), 2.16 (s, 6 H, *p*-Me), 2.12 ppm (s, 12 H, *o*-Me). **^{13}C{^{1}H} NMR** ($CDCl_3$): δ = 161.5 (N_2C), 138.7, 138.3 (2× C_{quat} Mes), 129.4 (CH Mes), 126.1 (C_{quat} Mes), 91.0 (cyclopentadienyl C_{ipso}), 72.2, 68.6 (cyclopentadienyl CH), 56.2 (CH_2), 20.9 (*p*-Me), 20.6 ppm (*o*-Me). $C_{31}H_{35}N_2ClFe$ (526.92): calcd. C 70.66, H 6.70, N 5.32%; found: C 69.48, H 6.91, N 4.87%.

Synthesis of 1^{Bn}S: A solution of $LiN(SiMe_3)_2$ (27 mg, 0.162 mmol) in THF (5 mL) was added dropwise to a stirred suspension of **1**^{Bn}H[BF_4] (80 mg, 0.162 mmol) and sulfur (10 mg, 0.31 mmol S) in THF (10 mL) at a bath temperature of −80 °C. After 1.5 h the cooling bath was removed and the stirred mixture was allowed to warm up to ambient temperature. After a further 1.5 h volatile components were removed under vacuum. The residue was subjected to purification by column chromatography (silica gel, dichloromethane), which furnished the crude product as a yellow powder. Subsequent recrystallisation from *n*-hexane afforded the product as yellow crystals. Yield 50 mg (70%). **^{1}H NMR** ($CDCl_3$): δ = 7.27 (m, 4 H, Ph), 7.21–7.13 (m, 6 H, Ph), 5.61 (s, 4 H, CH_2), 4.03, 3.76 ppm (2 s, 2× 4 H, C_5H_4). **^{13}C{^{1}H} NMR** ($CDCl_3$): δ = 187.3 (CS), 137.6 (C_{ipso} Ph), 128.3 (two closely spaced signals), 127.3 (3×CH Ph), 95.1 (cyclopentadienyl C_{ipso}), 71.2, 66.8 (2×cyclopentadienyl CH), 64.7 ppm (CH_2). $C_{25}H_{22}N_2SFe$ (438.37): C 68.50, H 5.06, N 6.39, S 7.31%; found: C 68.61, H 4.96, N 6.06, S 7.21%.

Synthesis of 1^{Bn*}S: Cold THF (2 mL) was added to **1**^{Bn*}H[BF_4] (67 mg, 0.116 mmol), $LiN(SiMe_3)_2$ (20 mg, 0.120 mmol) and sulfur (8 mg, 0.249 mmol S) at a bath temperature of −60 °C. After 5 min the cooling bath was removed and the stirred mixture was allowed to warm up to ambient temperature. Volatile components were removed under vacuum. The crude product was subjected to purification by column chromatography (silica gel, dichloromethane), which afforded the product as a yellow powder. Yield 53 mg (87%). **^{1}H NMR** ($CDCl_3$): δ = 6.70 (s, 4 H, $C_6H_2Me_3$), 5.69 (s, 4 H, CH_2), 3.94, 3.60 (2 s, 2×4 H, C_5H_4), 2.19 (s, 6 H, *p*-Me), 2.17 ppm (s, 12 H, *o*-Me). **^{13}C{^{1}H} NMR** ($CDCl_3$): δ = 186.6 (CS), 138.4, 137.1, 131.2 (3× C_{quat} Mes), 128.9 (CH Mes), 92.9 (cyclopentadienyl C_{ipso}), 70.8, 67.1, 57.8 (2×cyclopentadienyl CH and CH_2), 21.1 (*p*-Me), 20.1 ppm (*o*-Me). $C_{31}H_{34}N_2FeS$ (522.53): calcd. C 71.26, H 6.56, N 5.36, S 6.14%; found: C 71.60, H, 6.50, N 5.14, S 6.60%.

Synthesis of 1^{Bn}Se: Cold THF (2 mL) was added at a bath temperature of −60 °C to **1**^{Bn}H[BF_4] (110 mg, 0.223 mmol), $LiN(SiMe_3)_2$ (37 mg, 0.221 mmol) and grey selenium (37 mg, 0.469 mmol). The

 © 2022 The Authors. Zeitschrift für anorganische und allgemeine Chemie published by Wiley-VCH GmbH

stirred mixture was allowed to warm up to ambient temperature over the course of 2 h. Volatile components were removed under vacuum. The residue was subjected to purification by column chromatography (silica gel, dichloromethane), which afforded the product as a yellow powder. Yield 70 mg (65 %). **^{1}H NMR** (acetone-d_6): δ = 7.42 (m, 4 H, Ph), 7.32–7.24 (m, 6 H, Ph), 5.92 (s, 4 H, CH_2), 4.18, 4.05 ppm (2 s, 2×4 H, C_5H_4). **^{13}C{^{1}H} NMR** (acetone-d_6): δ = 189.8 (CSe), 138.3 (C_{ipso} Ph), 128.9, 128.0 (2×CH Ph), 96.4 (cyclopentadienyl C_{ipso}), 72.0, 69.0, 67.3 ppm (2×cyclopentadienyl CH and CH_2). **^{77}Se NMR** (acetone-d_6): δ = 321 ppm. $C_{25}H_{22}N_2FeSe$ (485.26): calcd. C 61.88, H 4.57, N 5.77 %; found: C 61.83, H 4.85, N 5.38 %.

Synthesis of 1^{Bn*}Se: THF (10 mL) was added to 1^{Bn*}H[BF_4] (101 mg, 0.175 mmol), LiN($SiMe_3$)$_2$ (29 mg, 0.173 mmol) and grey selenium (38 mg, 0.481 mmol). The mixture was stirred for 30 min. Volatile components were removed under vacuum. Toluene (15 mL) was added to the residue. Insoluble material was removed by filtration through a Celite pad and washed with toluene (3×3 mL). The washing solutions and filtrate were combined and reduced to dryness under vacuum. The crude product was subjected to purification by column chromatography (silica gel, dichloromethane), which afforded the product as a yellow powder. Yield 75 mg (76 %). **^{1}H NMR** ($CDCl_3$): δ = 6.70 (br. s, 4 H, $C_6H_2Me_3$), 5.82 (br. s, 4 H, CH_2), 3.95, 3.61 (2 br. s, 2×4 H, C_5H_4) 2.18 ppm (br. s, 18 H, Me). **^{13}C{^{1}H} NMR** ($CDCl_3$): δ = 187.0 (CSe), 138.3, 137.1, 130.9 (3×C_{quat} Mes), 128.8 (CH Mes), 93.2 (cyclopentadienyl C_{ipso}), 70.7, 66.7, 62.1 (2×cyclopentadienyl CH and CH_2), 20.9 (*p*-Me), 20.2 ppm (*o*-Me). **^{77}Se NMR** (acetone-d_6): δ = 359 ppm. $C_{31}H_{34}N_2FeSe$ (569.42): calcd. C 65.39, H 6.02, N 4.92 %; found: C 64.82, H, 6.01, N 4.81 %.

Synthesis of *cis*-[RhCl(CO)$_2$(1^{Bn})]: Cold toluene (3 mL) was added to 1^{Bn}H[BF_4] (50 mg, 0.101 mmol), LiN($SiMe_3$)$_2$ (17 mg, 0.102 mmol) and [Rh(μ-Cl)(COD)]$_2$ (26 mg, 0.050 mmol) at a bath temperature of −60 °C. The stirred mixture was allowed to warm up slowly to ambient temperature together with the cooling bath, leading to a colour change from yellow to red. Stirring was discontinued after 14 h. Insoluble material was removed by filtration through a Celite pad and washed with toluene (3×0.5 mL). The washing solutions and filtrate were combined. The atmosphere was exchanged from dinitrogen to carbon monoxide by freeze-pump-thaw cycles and the solution was subsequently stirred for 3 h, leading to a colour change from red to orange. Volatile components were removed under vacuum. The residue was subjected to purification by column chromatography (silica gel, dichloromethane), which afforded the product as a yellow powder. Yield 27 mg (45 %). **^{1}H NMR** ($CDCl_3$): δ = 7.35–7.28 (m, 10 H, Ph), 6.50, 5.36 (2 d, $^2J_{HH}$ = 14.4 Hz, 2×2 H, CH_2), 4.12, 4.07, 4.05, 3.76 (4 s, 4×2 H, C_5H_4). **^{13}C{^{1}H} NMR** ($CDCl_3$): δ = 211.0 (d, $^1J_{RhC}$ = 38.8 Hz, N_2C), 186.1 (d, $^1J_{RhC}$ = 54.4 Hz, RhCO), 183.4 (d, $^1J_{RhC}$ 76.8 Hz, RhCO), 135.9 (C_{ipso} Ph), 128.9, 128.6, 128.2 (3×CH Ph), 96.7 (cyclopentadienyl C_{ipso}), 71.3, 67.1 (2×cyclopentadienyl CH), 65.4 (CH_2). **IR** (CH_2Cl_2): $\tilde{\nu}$(CO) = 2081, 2001 cm^{-1}. $C_{27}H_{22}N_2ClFeO_2Rh$ (600.68): calcd. C 53.99, H 3.69, N 4.66 %; found: C 53.63, H 3.83, N 3.85 %.

Synthesis of *cis*-[RhCl(CO)$_2$(1^{Bn*})]: Cold toluene (3 mL) was added to 1^{Bn*}H[BF_4] (50 mg, 0.086 mmol), LiN($SiMe_3$)$_2$ (14 mg, 0.084 mmol) and [Rh(μ-Cl)(COD)]$_2$ (21 mg, 0.042 mmol) at a bath temperature of −60 °C. The stirred mixture was allowed to warm up slowly to ambient temperature together with the cooling bath, leading to a colour change from yellow to red. Stirring was discontinued after 14 h. Insoluble material was removed by filtration through a Celite pad and washed with toluene (3×0.5 mL). The washing solutions and filtrate were combined. The atmosphere was exchanged from dinitrogen to carbon monoxide by freeze-pump-thaw cycles and the solution was subsequently stirred for 1 h, leading to a colour change from red to orange. Volatile components were removed under vacuum. The residue was subjected to purification by column chromatography (silica gel, dichloromethane), which afforded the product as a yellow powder. Yield 36 mg (63 %). **^{1}H NMR** ($CDCl_3$): δ = 6.72 (s, 4 H, $C_6H_2Me_3$), 6.28, 5.19 (2 d, $^2J_{HH}$ = 13.6 Hz, 2×2 H, CH_2), 4.20, 4.03, 3.83, 3.40 (4 s, 4×2 H, C_5H_4), 2.26 (br. s, 12 H, *o*-Me), 2.19 ppm (s, 6 H, *p*-Me). **^{13}C{^{1}H} NMR** ($CDCl_3$): δ = 214.7 (d, $^1J_{RhC}$ = 39.4 Hz, N_2C), 186.5 (d, $^1J_{RhC}$ = 54.2 Hz, RhCO), 184.2 (d, $^1J_{RhC}$ = 76.9 Hz, RhCO), 138.4, 137.8, 129.3 (3×C_{quat} Mes), 129.1 (CH Mes), 95.5 (cyclopentadienyl C_{ipso}), 70.8, 70.5, 67.1, 66.8 (cyclopentadienyl CH), 60.0 (CH_2), 21.1 (*p*-Me), 20.6 ppm (*o*-Me). **IR** (CH_2Cl_2): $\tilde{\nu}$(CO) = 2078, 1998 cm^{-1}. $C_{33}H_{34}N_2ClFeO_2Rh$ (684.84): calcd. C 57.88, H 5.00, N 4.09 %; found: C 57.42, H 5.31, N 3.92 %.

Synthesis of [AuCl(1^{Bn*})]: Toluene (2 mL) was added to 1^{Bn*}H[BF_4] (29 mg, 0.050 mmol) and LiN($SiMe_3$)$_2$ (9 mg, 0.054 mmol). The mixture was stirred for 15 min. Insoluble material was removed by filtration through a Celite pad. The stirred filtrate was cooled to −60 °C. [AuCl(THT)] (16 mg, 0.050 mmol) was added. The stirred mixture was allowed to warm up slowly to ambient temperature together with the cooling bath. Stirring was discontinued after 14 h. Insoluble material was removed by filtration through a Celite pad and washed with THF (2×1 mL). The washing solutions and filtrate were combined. Volatile components were removed under vacuum, leaving the product as a yellow powder. Yield 29 mg (80 %). **^{1}H NMR** (CD_2Cl_2): δ = 6.76 (s, 4 H, $C_6H_2Me_3$), 5.90 (s, 4 H, CH_2), 4.04, 3.74 (2 s, 2×4 H, C_5H_4), 2.26 (s, 12 H, *o*-Me), 2.22 (s, 6 H, *p*-Me). **^{13}C{^{1}H} NMR** (CD_2Cl_2): δ = 202.7 (N_2C), 138.4, 129.0, 128.9 (3×$C_6H_2Me_3$), 94.5 (cyclopentadienyl C_{ipso}), 71.1, 67.0 (2×cyclopentadienyl CH), 61.1 (CH_2), 20.6 (two very closely spaced signals, 2×Me). $C_{31}H_{34}N_2AuClFe{\cdot}C_7H_8$ (815.02): calcd. C 56.00, H 5.19, N 3.44 %; found: C 56.46, H 5.56, N 3.44 %.

Synthesis of [CuBr(1^{Bn})]: Cold THF (3 mL) was added to 1^{Bn}H[BF_4] (33 mg, 0.067 mmol), LiN($SiMe_3$)$_2$ (11 mg, 0.066 mmol) and [CuBr(SMe_2)] (14 mg, 0.068 mmol) cooled to −60 °C. The stirred mixture was allowed to warm up slowly to ambient temperature together with the cooling bath. Stirring was discontinued after 14 h. Volatile components were removed under vacuum. Benzene (0.7 mL) was added. Insoluble material was removed by filtration and the filtrate stored at ambient temperature for 2 h, leading to the formation of yellow crystals. The mother liquor was separated off and layered with *n*-hexane (2.5 mL) to afford a second crop. The yellow crystals, which had formed over the course of 48 h, were isolated by decanting the mother liquor off. Yield 15 mg (41 %). **^{1}H NMR** (C_6D_6): δ = 7.49 (d, *J* = 7.4 Hz, 4 H, Ph), 7.12–7.04 (m, 6 H, Ph), 5.30 (s, 4 H, CH_2), 3.65, 3.35 (2 s, 2×4 H, C_5H_4). **^{13}C{^{1}H} NMR** (C_6D_6): δ = 212.7 (N_2C), 136.8 (C_{ipso} Ph), 129.7, 128.7, 128.4 (3×CH Ph), 97.2 (cyclopentadienyl C_{ipso}), 71.0, 67.2 (2×cyclopentadienyl CH), 66.4 (CH_2). $C_{25}H_{22}N_2BrCuFe{\cdot}C_6H_6$ (627.86): calcd. C 59.30, H 4.49, N 4.46 %; found: C 57.83, H 4.69, N 4.27 %.

X-ray Crystallography: For each data collection a single crystal was mounted on a micro-mount at 100(2) K, and all geometric and intensity data were taken from this sample, except for 1^{Bn*}HCl, which was measured at 250 K due to a phase transition at lower temperature. Data collections were carried out either on a Stoe IPDS2 diffractometer equipped with a 2-circle goniometer and an area detector or on a Stoe StadiVari diffractometer equipped with a 4-circle goniometer and a DECTRIS Pilatus 200 K detector. The data sets were corrected for absorption, Lorentz and polarisation effects. The structures were solved by direct methods (SHELXT) and refined using alternating cycles of least-squares refinements against F^2 (SHELXL2014/7).[58] H atoms were included in the models in calculated positions. H atoms involved in the short contacts indicated by dashed lines in Figures 5, 6 and 8–13 were found in the difference Fourier maps. All H atoms were treated with the 1.2 fold or 1.5 fold isotropic displacement parameter of their bonding partner. Experimental details for each diffraction experiment are given in Table 2.

 © 2022 The Authors. Zeitschrift für anorganische und allgemeine Chemie published by Wiley-VCH GmbH

Table 2. X-ray crystallographic details.

	3 b	**4 b**	$1^{Bn}H[BF_4]$	$1^{Bn*}H[BF_4]\cdot THF$	$1^{Bn*}HCl$	1^{Bn*}	$1^{Bn}Se$
Empirical formula	$C_{30}H_{32}FeN_2$	$C_{30}H_{36}FeN_2$	$C_{25}H_{23}BF_4FeN_2$	$C_{35}H_{43}BF_4FeN_2O$	$C_{31}H_{35}ClFeN_2$	$C_{31}H_{34}FeN_2$	$C_{25}H_{22}FeN_2Se$
Formula weight	476.42	480.46	494.11	650.37	526.91	490.45	485.25
Crystal system	monoclinic	monoclinic	orthorhombic	triclinic	monoclinic	monoclinic	triclinic
Space group	$P2_1/c$	$P2_1/c$	$P2_12_12_1$	P-1	$P2_1/n$	$P2_1/n$	P-1
a/Å	11.0809(6)	7.3687(3)	10.1217(4)	8.5917(8)	15.2852(6)	5.9423(4)	9.3479(5)
b/Å	20.8479(10)	28.4472(16)	21.3901(7)	13.4670(14)	19.5232(12)	15.426(2)	9.9536(5)
c/Å	11.3915(6)	5.7490(3)	10.2860(3)	14.0545(11)	22.2360(10)	26.7534(19)	21.7709(13)
α/°	90	90	90	83.394(7)	90	90	99.093(5)
β/°	116.398(4)	90.555(4)	90	78.151(7)	98.335(3)	95.760(6)	95.291(4)
γ/°	90	90	90	89.836(8)	90	90	89.998(4)
Volume/Å^3	2357.2(2)	1205.04(10)	2226.96(13)	1580.6(3)	6565.5(6)	2440.1(4)	1991.5(2)
Z	4	2	4	2	8	4	4
ρ_{calcd}/gcm^{-3}	1.342	1.324	1.474	1.367	1.066	1.335	1.618
μ/mm^{-1}	0.661	5.156	0.726	0.532	4.557	5.107	2.599
F(000)	1008.0	512.0	1016.0	684.0	2224.0	1040.0	984.0
Crystal size/mm^3	0.28×0.19×0.04	0.09×0.057×0.03	0.29×0.22×0.17	0.17×0.097×0.02	0.19×0.13×0.07	0.18×0.12×0.02	0.12×0.09×0.03
Radiation used	Mo-K_α (λ = 0.71073 Å)	Cu-K_α (λ = 1.54186 Å)	Mo-K_α (λ = 0.71073 Å)	Mo-K_α (λ = 0.71073 Å)	Cu-K_α (λ = 1.54186 Å)	Cu-K_α (λ = 1.54186 Å)	Mo-K_α (λ = 0.71073 Å)
2θ range for data collection/°	3.908–51.748	6.214–142.19	4.394–51.254	4.006–57.988	6.052–137.996	6.622–139.93	3.806–51.534
Index ranges	$-13 \le h \le 12$ $-25 \le k \le 25$ $-12 \le l \le 13$	$-8 \le h \le 8$ $-33 \le k \le 33$ $-3 \le l \le 6$	$-12 \le h \le 12$ $-25 \le k \le 25$ $-10 \le l \le 12$	$-11 \le h \le 11$ $-18 \le k \le 18$ $-13 \le l \le 19$	$-18 \le h \le 7$ $-18 \le k \le 23$ $-24 \le l \le 26$	$-7 \le h \le 3$ $-13 \le k \le 18$ $-32 \le l \le 31$	$-10 \le h \le 11$ $-12 \le k \le 12$ $-26 \le l \le 26$
Reflections collected	11642	8402	10000	13584	29564	13005	14008
Independent reflections	4376 [R_{int} = 0.0367]	2265 [R_{int} = 0.0626]	4189 [R_{int} = 0.0306]	8178 [R_{int} = 0.0731]	11966 [R_{int} = 0.0797]	4509 [R_{int} = 0.0794]	7483 [R_{int} = 0.0496]
Data/restraints/parameters	4376/0/304	2265/0/154	4189/0/298	8178/0/416	11966/24/644	4509/0/313	7483/0/523
Goodness-of-fit on F^2	1.031	1.176	1.039	1.041	1.020	1.053	1.050
Final R indexes	R_1 = 0.0508	R_1 = 0.0718	R_1 = 0.0264	R_1 = 0.0846	R_1 = 0.0954	R_1 = 0.0466	R_1 = 0.0494
[$I > 2\sigma(I)$]	wR_2 = 0.1258	wR_2 = 0.1835	wR_2 = 0.0709	wR_2 = 0.1975	wR_2 = 0.2417	wR_2 = 0.1207	wR_2 = 0.1269
Final R indexes	R_1 = 0.0734	R_1 = 0.0978	R_1 = 0.0278	R_1 = 0.1429	R_1 = 0.1803	R_1 = 0.0567	R_1 = 0.0762
[all data]	wR_2 = 0.1428	wR_2 = 0.1975	wR_2 = 0.0725	wR_2 = 0.2339	wR_2 = 0.3479	wR_2 = 0.1294	wR_2 = 0.1456
Residual electron density/eÅ^{-3}	0.37/−0.70	0.32/−0.37	0.28/−0.21	0.79/−1.14	0.43/−0.44	0.46/−0.39	0.69/−0.79
Flack parameter			−0.002(13)				
	$1^{Bn*}Se$	$1^{Bn}S$	$1^{Bn*}S$	*cis*-[RhCl(CO)$_2$(1^{Bn*})]	*cis*-[RhCl(CO)$_2$(1^{Bn})]	[AuCl(1^{Bn*})]	[CuBr(1^{Bn})]·C_6H_6
Empirical formula	$C_{31}H_{34}FeN_2Se$	$C_{25}H_{22}FeN_2S$	$C_{31}H_{34}FeN_2S$	$C_{33}H_{34}ClFFeN_2O_2Rh$	$C_{27}H_{22}ClFeN_2O_2Rh$	$C_{31}H_{34}AuClFeN_2$	$C_{31}H_{28}BrCuFeN_2$
Formula weight	569.41	438.35	522.51	703.83	600.67	722.87	627.85
Crystal system	monoclinic	monoclinic	monoclinic	triclinic	monoclinic	triclinic	monoclinic
Space group	$P2_1/c$	$C2/c$	$P2_1/c$	P-1	$P2_1/c$	P-1	$P2_1/n$
a/Å	6.4027(5)	7.9776(10)	6.3302(3)	8.7276(4)	20.499(4)	12.5069(8)	12.0990(5)
b/Å	30.1586(16)	17.1869(16)	30.1678(14)	9.4673(4)	6.2858(6)	14.8110(9)	10.0375(6)
c/Å	13.5418(8)	14.610(3)	13.3772(6)	19.1016(7)	18.712(2)	16.4857(10)	21.5491(10)
α/°	90	90	90	80.542(3)	90	68.483(5)	90
β/°	101.491(5)	92.534(12)	101.197(4)	84.669(3)	105.806(13)	75.601(5)	93.027(4)
γ/°	90	90	90	77.158(3)	90	81.462(5)	90
Volume/Å^3	2562.5(3)	2001.2(5)	2506.0(2)	1515.30(11)	2319.9(6)	2746.2(3)	2613.4(2)

 © 2022 The Authors. Zeitschrift für anorganische und allgemeine Chemie published by Wiley-VCH GmbH

Table 2. continued

Z	4	4	4	2	4	4	4
ρ_{calcd}/gcm^{-3}	1.476	1.455	1.385	1.543	1.720	1.748	1.596
μ/mm^{-1}	2.032	0.872	0.709	1.150	12.058	5.984	7.411
F(000)	1176.0	912.0	1104.0	718.0	1208.0	1424.0	1272.0
Crystal size/mm^3	0.6×0.56×0.481	0.09×0.07×0.04	0.13×0.09×0.06	0.19×0.16×0.12	0.22×0.107×0.03	0.29×0.19×0.07	0.2×0.15×0.09
Radiation used	Mo-K_α (λ = 0.71073 Å)	Mo-K_α (λ = 0.71073 Å)	Mo-K_α (λ = 0.71073 Å)	Mo-K_α (λ = 0.71073 Å)	Cu-K_α (λ = 1.54186 Å)	Mo-K_α (λ = 0.71073 Å)	Cu-K_α (λ = 1.54186 Å)
2θ range for data collection/°	5.084–61.762	4.74–51.54	2.7–51.446	4.462–65.462	8.968–143.056	2.716–51.706	8.202–143.434
Index ranges	$-9 \le h \le 8$	$-8 \le h \le 9$	$-7 \le h \le 5$	$-13 \le h \le 12$	$-24 \le h \le 21$	$-15 \le h \le 15$	$-11 \le h \le 14$
	$-42 \le k \le 41$	$-20 \le k \le 20$	$-33 \le k \le 36$	$-12 \le k \le 14$	$-7 \le k \le 4$	$-18 \le k \le 18$	$-10 \le k \le 12$
	$-19 \le l \le 17$	$-17 \le l \le 17$	$-16 \le l \le 16$	$-25 \le l \le 28$	$-22 \le l \le 22$	$-20 \le l \le 20$	$-26 \le l \le 15$
Reflections collected	12678	4614	12293	17195	10239	21906	13347
Independent reflections	7222 [R_{int} = 0.0373]	1891 [R_{int} = 0.0330]	4740 [R_{int} = 0.0434]	9232 [R_{int} = 0.0327]	4410 [R_{int} = 0.0490]	10488 [R_{int} = 0.0398]	4965 [R_{int} = 0.0170]
Data/restraints/parameters	7222/0/322	1891/0/133	4740/0/322	9232/0/367	4410/0/307	10488/0/661	4965/0/325
Goodness-of-fit on F^2	1.026	1.132	1.035	1.034	1.093	1.035	1.049
Final R indexes	R_1 = 0.0433	R_1 = 0.0404	R_1 = 0.0360	R_1 = 0.0441	R_1 = 0.0557	R_1 = 0.0339	R_1 = 0.0275
[$I > 2\sigma(I)$]	wR_2 = 0.1156	wR_2 = 0.0981	wR_2 = 0.0895	wR_2 = 0.1153	wR_2 = 0.1580	wR_2 = 0.0840	wR_2 = 0.0687
Final R indexes	R_1 = 0.0610	R_1 = 0.0557	R_1 = 0.0476	R_1 = 0.0604	R_1 = 0.0671	R_1 = 0.0444	R_1 = 0.0319
[all data]	wR_2 = 0.1235	wR_2 = 0.1059	wR_2 = 0.0953	wR_2 = 0.1244	wR_2 = 0.1687	wR_2 = 0.0879	wR_2 = 0.0728
Residual electron density/eÅ^{-3}	0.76/−0.59	0.66/−0.26	0.33/−0.28	1.16/−0.65	1.15/−1.50	2.27/−1.59	0.31/−0.47
Flack parameter							

Crystallographic data (excluding structure factors) for the structures in this paper have been deposited with the Cambridge Crystallographic Data Centre, CCDC, 12 Union Road, Cambridge CB21EZ, UK. Copies of the data can be obtained free of charge on quoting the depository numbers CCDC-2212529 (**4b**), CCDC-2212530 (**4b**), CCDC-2212531 (**1**^{Bn}H[BF_4]), CCDC-2212532 (**1**^{Bn*}H[BF_4]·THF), CCDC-2212533 (**1**^{Bn*}HCl), CCDC-2212534 (**1**^{Bn*}), CCDC-2212535 (**1**^{Bn}Se), CCDC-2212536 (**1**^{Bn*}Se), CCDC-2212537 (**1**^{Bn}S), CCDC-2212538 (**1**^{Bn*}S), CCDC-2212539 (*cis*-[RhCl(CO)$_2$(**1**^{Bn*})]), CCDC-2212540 (*cis*-[RhCl(CO)$_2$(**1**^{Bn})]), CCDC-2212541 ([AuCl(**1**^{Bn*})]), and CCDC-2212542 ([CuBr(**1**^{Bn})]·C_6H_6).

Acknowledgements

Open Access funding enabled and organized by Projekt DEAL.

Conflict of Interest

The authors declare no conflict of interest.

Data Availability Statement

The data that support the findings of this study are available in the supplementary material of this article.

Keywords: Carbenes · Gold · Metallocenes · Rhodium · Selenium

[1] a) C. D. Varnado Jr., E. L. Rosen, M. S. Collins, V. M. Lynch, C. W. Bielawski, *Dalton Trans.* **2013**, *42*, 13251–13264; b) E. L. Rosen, C. D. Varnado Jr., A. G. Tennyson, D. M. Khramov, J. W. Kamplain, D. H. Sung, P. T. Cresswell, V. M. Lynch, C. W. Bielawski, *Organometallics* **2009**, *28*, 6695–6706; c) D. M. Khramov, E. L. Rosen, V. M. Lynch, C. W. Bielawski, *Angew. Chem. Int. Ed.* **2008**, *47*, 2267–2270; *Angew. Chem.* **2008**, *120*, 2299–2302.

[2] Recent reviews: a) Y. Ryu, G. Ahumada, C. W. Bielawski, *Chem. Commun.* **2019**, *55*, 4451–4466; b) E. Peris, *Chem. Rev.* **2018**, *118*, 9988–10031.

[3] Seminal papers: a) N. Matsumura, J.-i. Kawano, N. Fukunishi, H. Inoue, *J. Am. Chem. Soc.* **1995**, *117*, 3523–3624; b) R. W. Alder, M. E. Blake, C. Bortolotti, S. Bufali, C. P. Butts, E. Linehan, J. M. Oliva, A. G. Orpen, M. J. Quayle, *Chem. Commun.* **1999**, 241–242; selected recent references: c) G. Kundu, V. S. Ajithkumar, K. V. Raj, K. Vanka, S. Tothadi, S. S. Sen, *Chem. Commun.* **2022**, *58*, 3783–3786; d) W. J. M. Blackaby, K. L. M. Harriman, S. M. Greer, A. Folli, S. Hill, V. Krewald, M. F. Mahon, D. M. Murphy, M. Murugesu, E. Richards, S. Suturina, M. K. Whittlesey, *Inorg. Chem.* **2022**, *61*, 1308–1315; e) Y. Ma, H. Saqib Ali, A. A. Hussein, *Catal. Sci. Technol.* **2022**, *12*, 674–685; f) R. S. C. Charman, M. F. Mahon, J. P. Lowe, D. J. Liptrot, *Dalton Trans.* **2022**, *51*, 831–835; g) K. Mori, M. Akiyama, K. Inada, Y. Imamura, Y. Ishibashi, Y. Takahira, K. Nozaki, T. Okazoe, *J. Am. Chem. Soc.* **2021**, *143*, 20980–20987; h) M. E. Grundy, K. Yuan, G. S. Nichol, M. J. Ingleson, *Chem. Sci.* **2021**, *12*, 8190–8198; i) S. A. Rzhevskiy, A. N. Philippova, G. A. Chesnokov, A. A. Ageshina, L. I. Minaeva, M. A. Topchiy, M. S. Nechaev, A. F. Asachenko, *Chem. Commun.* **2021**, *57*, 5686–5689; j) A. Cer-

 © 2022 The Authors. Zeitschrift für anorganische und allgemeine Chemie published by Wiley-VCH GmbH

vantes-Reyes, T. Saxl, P. M. Stein, M. Rudolph, F. Rominger, A. M. Asiri, A. S. K. Hashmi, *ChemSusChem* **2021**, *14*, 2367–2374; k) S. L. Strausser, D. M. Jenkins, *Organometallics* **2021**, *40*, 1706–1712; l) J. W. Hall, D. Bouchet, M. F. Mahon, M. K. Whittlesey, C. S. J. Cazin, *Organometallics* **2021**, *40*, 1252–1261; m) S. Takebayashi, R. R. Fayzullin, *Organometallics* **2021**, *40*, 500–507; n) M. J. Benedikter, J. V. Musso, W. Frey, R. Schowner, M. R. Buchmeiser, *Angew. Chem. Int. Ed.* **2021**, *60*, 1374–1382; *Angew. Chem.* **2021**, *133*, 1394–1402.

[4] See, for example: a) M. C. Jahnke, F. E. Hahn, in *N-Heterocyclic Carbenes* (Ed.: S. Díez-González), Royal Society of Chemistry, Cambridge, **2011**, pp. 1–41; b) F. E. Hahn, M. C. Jahnke, *Angew. Chem. Int. Ed.* **2008**, *47*, 3122–3172; *Angew. Chem.* **2008**, *120*, 3166–3216; c) D. Bourissou, O. Guerret, F. P. Gabbaï, G. Bertrand, *Chem. Rev.* **2000**, *100*, 39–91.

[5] a) L. Wallbaum, D. Weismann, D. Löber, C. Bruhn, P. Prochnow, J. E. Bandow, U. Siemeling, *Chem. Eur. J.* **2019**, *25*, 1488–1497; b) T. Schulz, D. Weismann, L. Wallbaum, R. Guthardt, C. Thie, M. Leibold, C. Bruhn, U. Siemeling, *Chem. Eur. J.* **2015**, *21*, 14107–14121; c) M. S. Collins, E. L. Rosen, V. M. Lynch, C. W. Bielawski, *Organometallics* **2010**, *29*, 3047–3053; d) R. W. Alder, P. R. Allen, M. Murray, A. G. Orpen, *Angew. Chem. Int. Ed. Engl.* **1996**, *35*, 1121–1123.

[6] See, for example: a) A. Kumar, D. Yuan, H. V. Huynh, *Inorg. Chem.* **2019**, *58*, 7545–7553; b) C. M. Weinstein, G. P. Junor, D. R. Tolentino, R. Jazzar, M. Melaimi, G. Bertrand, *J. Am. Chem. Soc.* **2018**, *140*, 9255–9260; c) M. Iglesias, D. J. Beetstra, J. C. Knight, L.-L. Ooi, A. Stasch, S. Coles, L. Male, M. B. Hursthouse, K. J. Cavell, A. Dervisi, I. A. Fallis, *Organometallics* **2008**, *27*, 3279–3289.

[7] a) B. A. Correia Bicho, R. Guthardt, C. Bruhn, D. Großhennig, T. Orth, F. Pfeiffer, U. Siemeling, *Eur. J. Inorg. Chem.* **2022**, e202101014; b) A. R. Petrov, A. Derheim, J. Oetzel, M. Leibold, C. Bruhn, S. Scheerer, S. Oßwald, R. F. Winter, U. Siemeling, *Inorg. Chem.* **2015**, *54*, 6657–6670; c) S. Rittinghaus, C. Färber, C. Bruhn, U. Siemeling, *Dalton Trans.* **2014**, *43*, 3508–3520; d) U. Siemeling, C. Färber, M. Leibold, C. Bruhn, P. Mücke, R. F. Winter, B. Sarkar, M. von Hopffgarten, G. Frenking, *Eur. J. Inorg. Chem.* **2009**, 4607–4612; e) U. Siemeling, C. Färber, C. Bruhn, *Chem. Commun.* **2009**, 98–100.

[8] a) C. Goedecke, M. Leibold, U. Siemeling, G. Frenking, *J. Am. Chem. Soc.* **2011**, *133*, 3557–3569; b) U. Siemeling, C. Färber, C. Bruhn, M. Leibold, D. Selent, W. Baumann, M. von Hopffgarten, C. Goedecke, G. Frenking, *Chem. Sci.* **2010**, *1*, 697–704.

[9] For selected reviews, see: a) I. Alkorta, J. Elguero, *J. Heterocycl. Chem.* **2019**, *56*, 359–370; b) H. Song, Y. Kim, J. Park, K. Kim, E. Lee, *Synlett* **2016**, *27*, 477–485; c) S. Yadav, S. Saha, S. S. Sen, *ChemCatChem* **2016**, *8*, 486–501; d) U. Siemeling, *Aust. J. Chem.* **2011**, *64*, 1109–1112; e) D. Martin, M. Soleilhavoup, G. Bertrand, *Chem. Sci.* **2011**, *2*, 389–399.

[10] C. Thie, C. Bruhn, U. Siemeling, *Eur. J. Inorg. Chem.* **2015**, 5457–5466.

[11] This is the most widely used method to access suitable NHC precursors; see: L. Benhamou, E. Chardon, G. Lavigne, S. Bellemin-Laponnaz, V. César, *Chem. Rev.* **2011**, *111*, 2705–2733.

[12] V. C. Gibson, N. J. Long, E. L. Marshall, P. J. Oxford, A. J. P. White, D. J. Williams, *J. Chem. Soc. Dalton Trans.* **2001**, 1162–1164.

[13] For selected reviews, see: a) M. Nishio, *Phys. Chem. Chem. Phys.* **2011**, *13*, 13873–13900; b) M. Nishio, Y. Umezawa, K. Honda, S. Tsuboyama, H. Suezawa, *CrystEngComm* **2009**, *11*, 1757–1788; c) M. Nishio, *CrystEngComm* **2004**, *6*, 130–158; d) O. Takahashi, Y. Kohno, S. Iwasaki, K. Saito, M. Iwaoka, S. Tomoda, Y. Umezawa, S. Tsuboyama, M. Nishio, *Bull. Chem. Soc. Jpn.* **2001**, *74*, 2421–2430; e) for an example of an imidazolium $N_2CH\cdots\pi$(phenyl) interaction, see: J. Dupont, P. A. Z. Suarez, R. F. De Souza, R. A. Burrow, J.-P. Kintzinger, *Chem. Eur. J.* **2000**, *6*, 2377–2381.

[14] H. V. Huynh, T. T. Lam, H. T. T. Luong, *RSC Adv.* **2018**, *8*, 34960–34966.

[15] A. J. Arduengo III, R. L. Harlow, M. Kline, *J. Am. Chem. Soc.* **1991**, *113*, 361–363.

[16] D. Tapu, D. A. Dixon, C. Roe, *Chem. Rev.* **2009**, *109*, 3385–3407.

[17] a) B.-M. Yang, K. Xiang, Y.-Q. Tu, S.-H. Zhang, D.-T. Yang, S.-H. Wang, F.-M. Zhang, *Chem. Commun.* **2014**, *50*, 7163–7165; b) S. Kronig, E. Theuergarten, D. Holschumacher, T. Bannenberg, C. G. Daniliuc, P. G. Jones, M. Tamm, *Inorg. Chem.* **2011**, *50*, 7344–7359; c) M. Iglesias, D. J. Beetstra, J. C. Knight, L.-L Ooi, A. Stasch, S. Coels, L. Male, M. B. Hursthouse, K. J. Cavell, A. Dervisi, I. A. Fallis, *Organometallics* **2008**, *27*, 3279–3289; d) P. Bazinet, G. P. A. Yap, D. S. Richeson, *J. Am. Chem. Soc.* **2003**, *125*, 13314–13315.

[18] E. L. Rosen, D. H. Sung, Z. Chen, V. M. Lynch, C. W. Bielawski, *Organometallics* **2010**, *29*, 250–256.

[19] M. Nonnenmacher, D. Kunz, F. Rominger, T. Oeser, *Chem. Commun.* **2006**, 1378–1380.

[20] D. Munz, *Organometallics* **2018**, *37*, 275–289.

[21] F. Mendez, M. A. Garcia-Garibay, *J. Org. Chem.* **1999**, *64*, 7061–7066.

[22] Seminal paper: a) R. D. Bach, M.-D. Su, E. Aldabbagh, J. L. Andrés, H. B. Schlegel, *J. Am. Chem. Soc.* **1993**, *115*, 10237–10246; for recent work, see ref. [6b] as well as: b) V. Lavallo, J. Mafhouz, Y. Canac, B. Donnadieu, W. W. Schoeller, G. Bertrand, *J. Am. Chem. Soc.* **2004**, *126*, 8670–8671.

[23] a) K. Verlinden, H. Buhl, W. Frank, C. Ganter, *Eur. J. Inorg. Chem.* **2015**, 2416–2425; b) D. M. Buck, D. Kunz, *Organometallics* **2015**, *34*, 5335–5340; see also: c) R. Weiss, S. Reichel, M. Handke, F. Hampel, *Angew. Chem. Int. Ed.* **1998**, *37*, 344–347; *Angew. Chem.* **1998**, *110*, 352–354.

[24] H. V. Huynh, *Chem. Rev.* **2018**, *118*, 9457–9492.

[25] Determination of these coupling constants from the ^{13}C satellites in the ^{1}H NMR spectra was hampered due to broadening of the formamidinium signal.

[26] $^{1}J_{CH}$ values of ca. 190 Hz have been reported for protonated five-membered CAACs; see: a) J. Volk, M. Heinz, M. Leibold, C. Bruhn, T. Bens, B. Sarkar, M. C. Holthausen, U. Siemeling, *Chem. Commun.* **2022**, *58*, 10396–10399; b) G. Meng, L. Kakalis, S. P. Nolan, M. Szostak, *Tetrahedron Lett.* **2019**, *60*, 378–381.

[27] E. Yu. Tupikina, G. S. Denisov, A. S. Antonov, P. M. Tolsoy, *Phys. Chem. Chem. Phys.* **2020**, *22*, 1994–2000.

[28] A. Liske, K. Verlinden, H. Buhl, K. Schaper, C. Ganter, *Organometallics* **2013**, *32*, 5269–5272.

[29] S. V. C. Vummaleti, D. J. Nelson, A. Poater, A. Gomez-Suarez, D. B. Cordes, A. M. Z. Slawin, S. P. Nolan, L. Cavallo, *Chem. Sci.* **2015**, *6*, 1895–1904.

[30] G. P. Junor, J. Lorkowski, C. M. Weinstein, R. Jazzar, C. Pietraszuk, G. Bertrand, *Angew. Chem. Int. Ed.* **2020**, *59*, 22028–22033; *Angew. Chem.* **2020**, *132*, 22212–22217.

[31] For the first observation of a CH···Se "hydrogen bond" (H···Se 2.92 Å, C–H–Se 102°), see: M. Iwaoka, S. Tomoda, *J. Am. Chem. Soc.* **1994**, *116*, 4463–4464.

[32] D. J. Nelson, A. Collado, S. Manzini, S. Meiries, A. M. Z. Slawin, D. B. Cordes, S. P. Nolan, *Organometallics* **2014**, *33*, 2048–2058.

[33] An exceptionally short C–Se bond of 1.788(5) Å has been reported for a particularly electrophilic cationic NHC with a tropylium-based backbone; see: S. Appel, P. Brüggemann, C. Ganter, *Chem. Commun.* **2020**, *56*, 9020–9023.

[34] E. Tomás-Mendivil, M. H. Hansmann, C. M. Weinstein, R. Jazzar, M. Melaimi, G. Bertrand, *J. Am. Chem. Soc.* **2017**, *139*, 7753–7756.

[35] For a comprehensive review of CH···S hydrogen bonding interactions, see: H. A. Fargher, T. J. Sherbow, M. M. Haley,

 © 2022 The Authors. Zeitschrift für anorganische und allgemeine Chemie published by Wiley-VCH GmbH

D. W. Johnson, M. D. Pluth, *Chem. Soc. Rev.* **2022**, *51*, 1454–1469.
[36] B. Cordero, V. Gómez, A. E. Platero-Prats, M. Revés, J. Echeverría, E. Cremades, F. Barragán, S. Alvarez, *Dalton Trans.* **2008**, 2832–2838.
[37] See, for example: a) Z.-J. Cai, C.-X. Liu, Q. Gu, S.-L. You, *Angew. Chem. Int. Ed.* **2018**, *57*, 1296–1299; *Angew. Chem.* **2018**, *130*, 1310–1313; b) R. Gleiter, B. Gaa, C. Sigwart, H. Lange, O. Borzyk, F. Rominger, H. Irngartinger, T. Oeser, *Eur. J. Org. Chem.* **1998**, 171–176; c) P. Jutzi, K.-H. Schwartzen, A. Mix, H.-G. Stammler, B. Neumann, *Chem. Ber.* **1993**, *126*, 415–420.
[38] See, for example: a) K. Okuma, K. Kojima, I. Kaneko, Y. Tsujimoto, H. Ohta, Y. Yokomori, *J. Chem. Soc. Perkin Trans. 1* **1994**, 2151–2159; b) P. R. Brooks, J. A. Counter, R. Bishop, E. R. T. Tiekink, *Acta Crystallogr. Sect. C* **1991**, *47*, 1939–1941.
[39] Recent reviews: a) S. Yadav, R. Deka, H. B. Singh, *Chem. Lett.* **2019**, *48*, 65–79; b) J. Ritch, *Phys. Sci. Rev.* **2019**, *4*, 20170128; see also:; c) A. Doddi, M. Peters, M. Tamm, *Chem. Rev.* **2019**, *119*, 6994–7112.
[40] For recent references, see: a) D. Sambade, C. Collins, G. Parkin, *J. Mol. Struct.* **2021**, *1231*, 129682; b) M. Saab, D. J. Nelson, N. V. Tzouras, T. A. C. A. Bayrakdah, S. P. Nolan, F. Nahra, K. Van Hecke, *Dalton Trans.* **2020**, *49*, 12068–12081.
[41] A value of 2035 cm^{-1} has been published for the $\mathbf{1}^{iBu}$ analogue; see ref. [1c].
[42] U. S. D. Paul, C. Sieck, M. Haehnel, K. Hammond, T. B. Marder, U. Radius, *Chem. Eur. J.* **2016**, *22*, 11005–11014.
[43] T. G. Appleton, H. C. Clark, L. E. Manzer, *Coord. Chem. Rev.* **1973**, *10*, 335–422.
[44] See, for example: a) K. A. Netland, A. Krivikapic, M. Tilset, *J. Coord. Chem.* **2010**, *63*, 2909–2927; b) J. Slattery, R. J. Thatcher, Q. Shi, R. E. Douthwaite, *Pure Appl. Chem.* **2010**, *82*, 1663–1671; c) M. Heckenroth, A. Neels, M. G. Garnier, P. Aebi, A. W. Ehlers, M. Albrecht, *Chem. Eur. J.* **2009**, *15*, 9375–9386.
[45] Reviews: a) M. Brookhart, M. L. H. Green, G. Parkin, *Proc. Natl. Acad. Sci. USA* **2007**, *104*, 6908–6914; b) L. Brammer, *Dalton Trans.* **2003**, 3145–3157; see also: c) W. Yao, O. Eisenstein, R. H. Crabtree, *Inorg. Chim. Acta* **1997**, *254*, 105–111.
[46] See, for example: a) J. E. Barquera-Lozada, A. Obenhuber, C. Hauf, W. Scherer, *J. Phys. Chem. A* **2013**, *117*, 4304–4315; b) Y. Zhang, J. C. Lewis, R. G. Bergman, J. A. Ellman, E. Oldfield, *Organometallics* **2006**, *25*, 3515–3519.
[47] a) L. Falivene, Z. Cao, A. Petta, L. Serra, A. Poater, R. Oliva, V. Scarano, L. Cavallo, *Nat. Chem.* **2019**, *11*, 872–879; b) A. Gómez-Suárez, D. J. Nelson, S. P. Nolan, *Chem. Commun.* **2017**, *53*, 2650–2660; c) H. Clavier, S. P. Nolan, *Chem. Commun.* **2010**, *46*, 841–861.
[48] J. J. Dunsford, K. J. Cavell, B. M. Kariuki, *Organometallics* **2012**, *31*, 4118–4121.
[49] F. Ragone, A. Poater, L. Cavallo, *J. Am. Chem. Soc.* **2010**, *132*, 4249–4258.
[50] Seminal paper introducing the concept of NHCs with flexible steric bulk: G. Altenhoff, R. Goddard, C. W. Lehmann, F. Glorius, *Angew. Chem. Int. Ed.* **2003**, *43*, 3690–3693.
[51] A. Collado, J. Balogh, S. Meiries, A. M. Z. Slawin, L. Falivene, L. Cavallo, S. P. Nolan, *Organometallics* **2013**, *32*, 3249–3252.
[52] See, for example: a) H. Hu, H. Ichiryu, K. Nakajima, M. Ogasawara, *ACS Omega* **2021**, *6*, 5981–5989; b) H. Salem, M. Schmitt, U. Herrlich (née Blumbach), E. Kühnel, M. Brill, P. Nägele, A. L. Bogado, F. Rominger, P. Hofmann, *Organometallics* **2013**, *32*, 29–46; c) M. J. Page, J. Wagler, B. A. Messerle, *Dalton Trans.* **2009**, 7029–7038; d) C. Rüchardt, H.-D. Beckhaus, *Angew. Chem. Int. Ed. Engl.* **1985**, *24*, 529–538.
[53] R. S. Holdroyd, M. J. Page, M. R. Warren, M. K. Whittlesey, *Tetrahedron Lett.* **2010**, *51*, 557–559.
[54] See, for example: a) J. L. Peltier, E. Tomás-Mendevil, D. R. Tolentino, M. M. Hansman, R. Jazzar, G. Bertrand, *J. Am. Chem. Soc.* **2020**, *142*, 18336–18340; b) L. E. Lieske, L. A. Freeman, G. Wang, D. A. Dickie, R. J. Gilliard, Jr., C. W. Machan, *Chem. Eur. J.* **2019**, *25*, 6098–6101; c) J. K. Mahoney, D. Martin, F. Thomas, C. E. Moore, A. L. Rheingold, G. Bertrand, *J. Am. Chem. Soc.* **2015**, *137*, 7519–7525; d) D. R. Anderson, V. Lavallo, D. J. O'Leary, G. Bertrand, R. H. Grubbs, *Angew. Chem. Int. Ed.* **2007**, *46*, 7262–7265; *Angew. Chem.* **2007**, *119*, 7400–7403; e) V. Lavallo, Y. Canac, B. Donnadieu, W. W. Schoeller, G. Bertrand, *Angew. Chem. Int. Ed.* **2006**, *45*, 3488–3491; *Angew. Chem.* **2006**, *118*, 3568–3571.
[55] R. Guthardt, J. Blanckenberg, C. Bruhn, U. Siemeling, *Chem. Commun.* **2021**, *57*, 12984–12987.
[56] R. Uson, A. Laguna, M. Laguna, D. A. Briggs, H. H. Murray, J. P. Fackler, Jr., *Inorg. Synth.* **1989**, *26*, 85–91.
[57] H. Duddeck, *Prog. Nucl. Magn. Reson. Spectrosc.* **1995**, *27*, 1–323.
[58] G. M. Sheldrick, *Acta Crystallogr. Sect. A* **2008**, *64*, 112–122.

Manuscript received: October 14, 2022
Revised manuscript received: December 1, 2022
Accepted manuscript online: December 8, 2022

 © 2022 The Authors. Zeitschrift für anorganische und allgemeine Chemie published by Wiley-VCH GmbH